Spacetime Interfacial Damage Model for Elastodynamic Fracture with Riemann Contact Conditions

Reza Abedi, Robert B. Haber
Department of Mechanical Science & Engineering
University of Illinois at Urbana–Champaign

16th U.S. National Congress of
Theoretical and Applied Mechanics
June 27 - July 2 2010

Features of spacetime discontinuous Galerkin finite element methods

- Inter-element discontinuous basis functions
  - Weak enforcement of balance/conservation jump conditions in spacetime (e.g., Rankine–Hugoniot conditions for conservation laws)
  - Enables exact conservation per element and O(N) complexity for hyperbolic problems

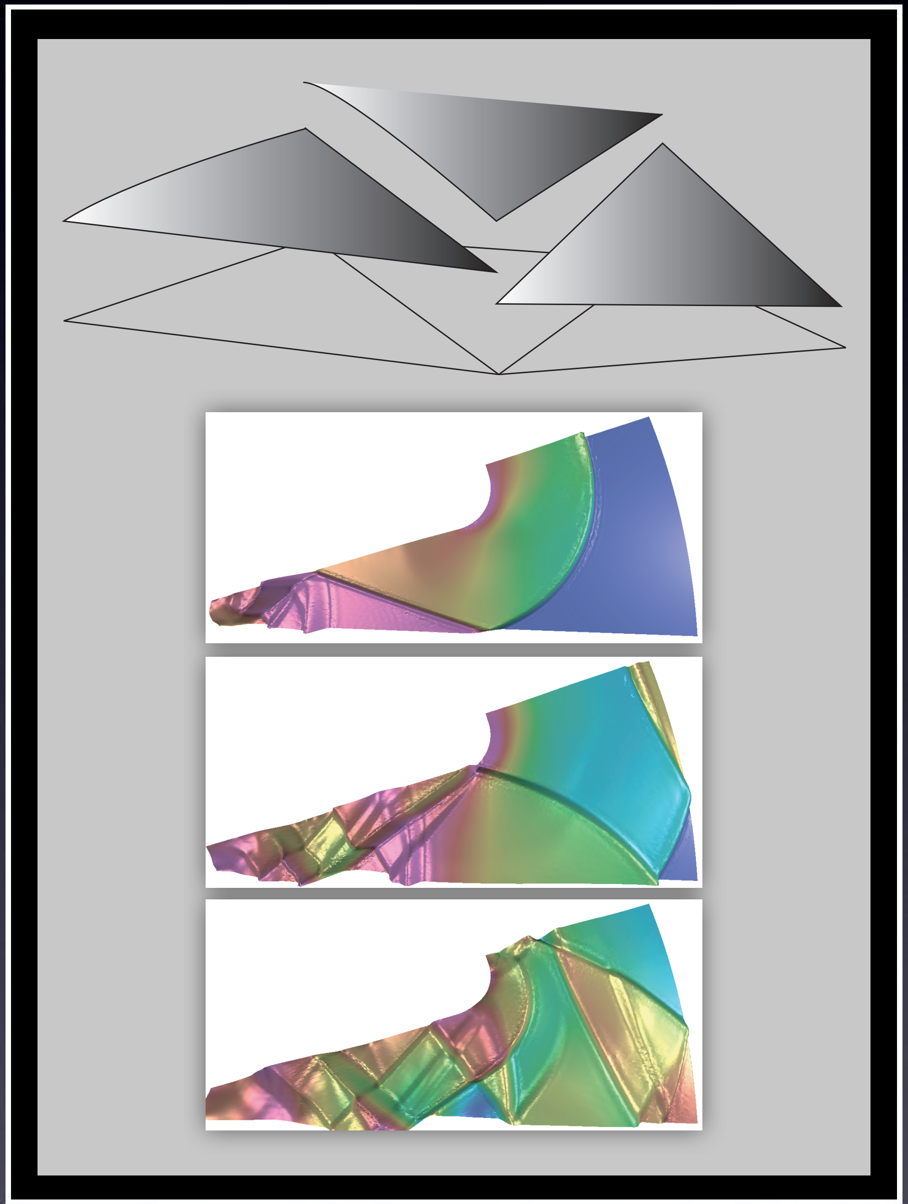

Features of spacetime discontinuous Galerkin finite element methods

- Direct discretization of spacetime
  - Replaces separate temporal integration
  - Unstructured spacetime mesh eliminates tangling in moving–boundary problems
  - Unambiguous numerical framework for initial/boundary conditions (vs. finite volume, finite difference)

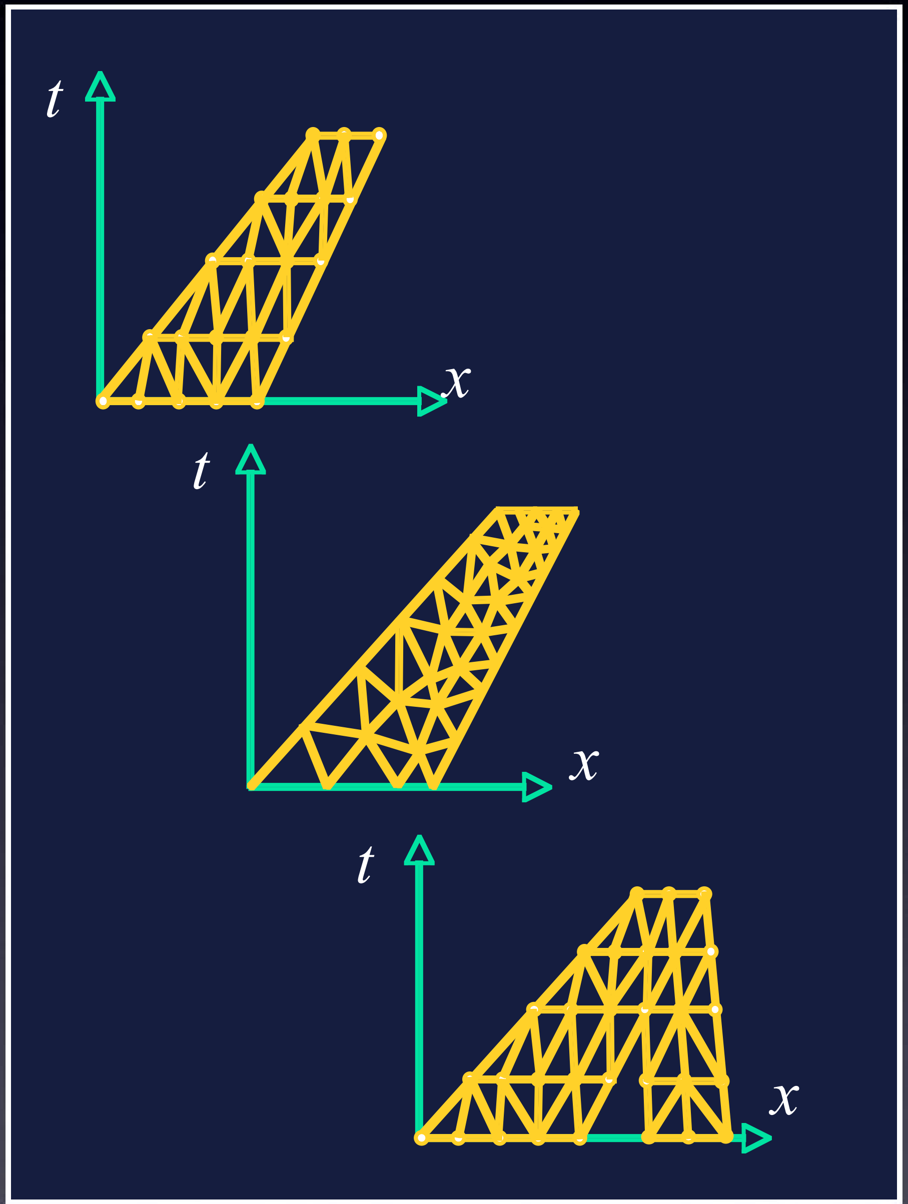

Causal Spacetime Mesh and O(*N*) Advancing-Front Solution Strategy

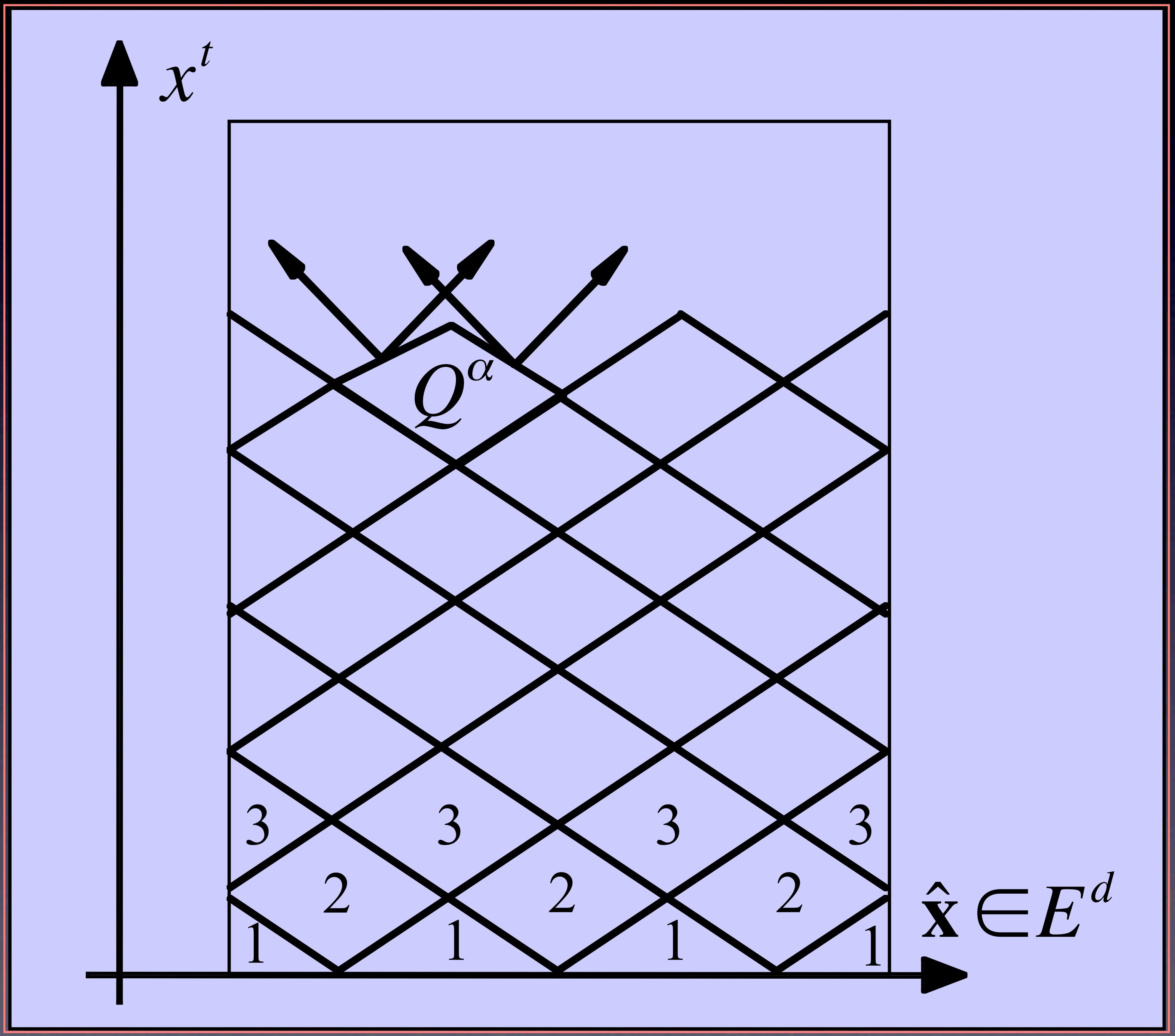

Tent Pitcher:
causal spacetime meshing

- Given a space mesh, Tent Pitcher constructs a spacetime mesh such that every facet on sequence of advancing fronts is spacelike (patch height bounded by *causality constraint*)
- Similar to CFL condition, except entirely *local* and not related to stability (required for O(*N*) solution)

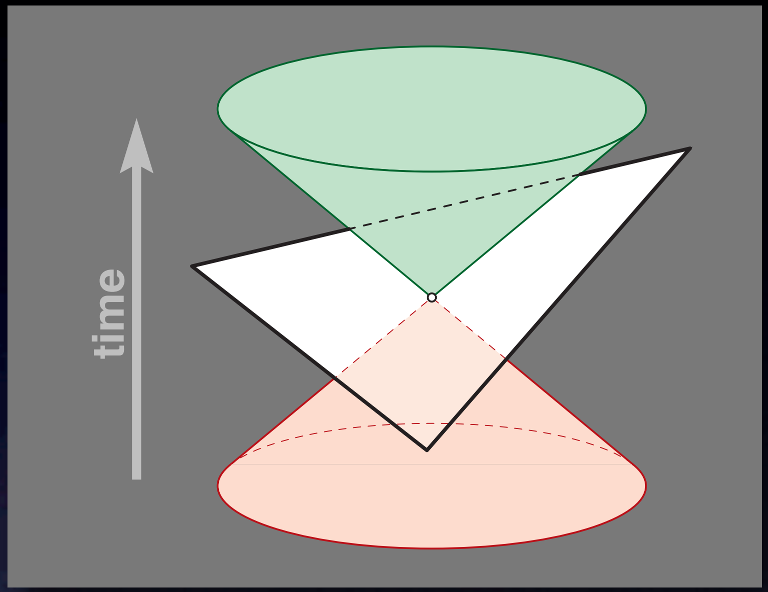

causality constraint

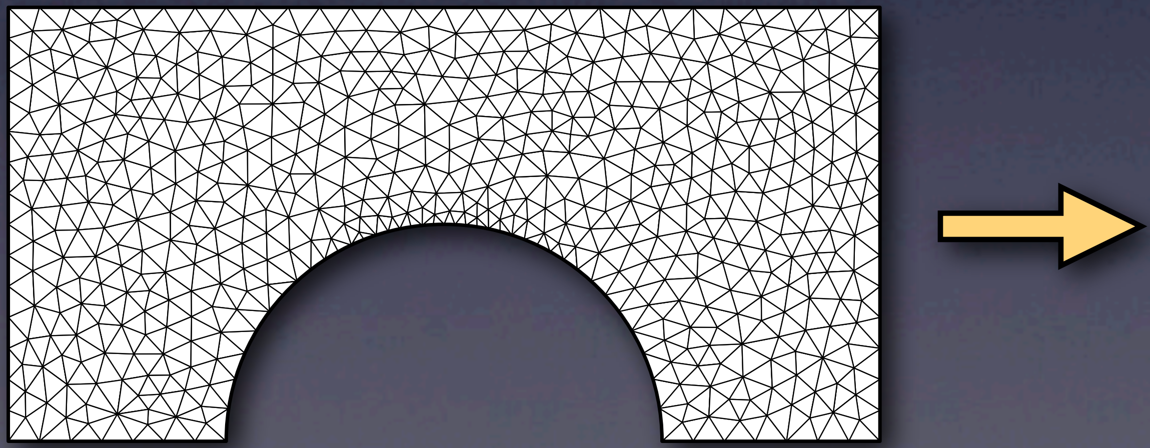

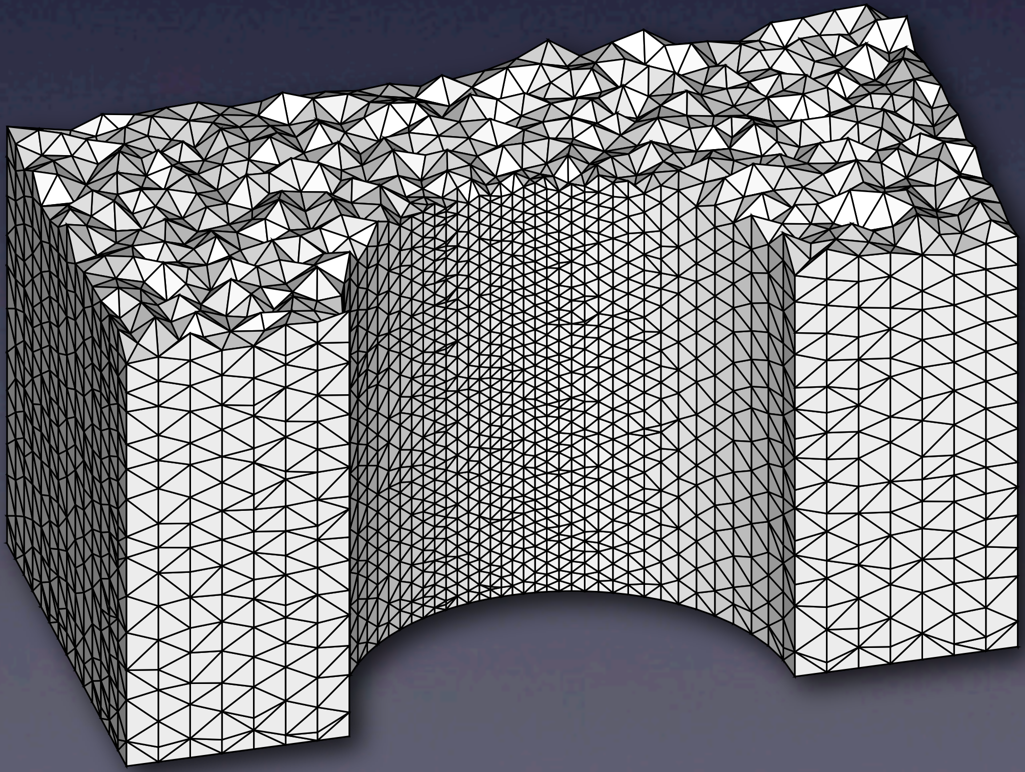

Tent Pitcher: patch–by–patch meshing & solution

- Patches ('tents') of tetrahedra; solve immediately for O(N) method with rich parallel structure
- Maintain "space mesh" as advancing, space-like front with non-uniform time coordinates

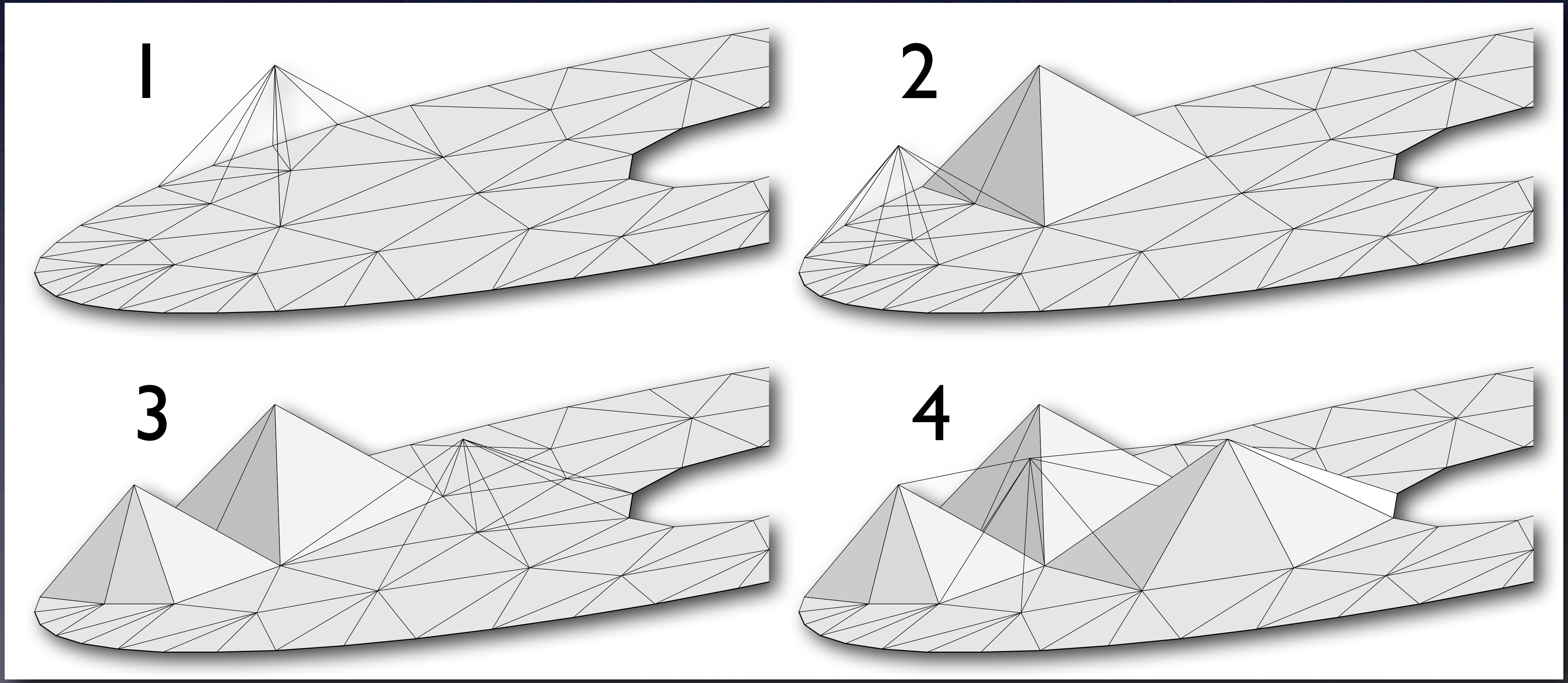

Force-like fields

(d,d+1-forms with vector coefficients)

- Body force ($(d+1)$-form): $\boldsymbol{b} = \mathbf{b}\boldsymbol{\Omega}$
- Spacetime momentum flux (d-form): $\boldsymbol{M} = \boldsymbol{p} - \boldsymbol{\sigma}$

  $\boldsymbol{M}|_{\Gamma} =$ linear momentum flux across $d-$manifold Γ

  - Linear momentum density: $\boldsymbol{p} = \mathbf{p}{\star}\mathrm{dt}$
  - Stress/traction: $\boldsymbol{\sigma} = \boldsymbol{\upsigma} \wedge \star\mathbf{dx}$
  - Stokes Theorem: $\int_{\partial \mathcal{Q}} \boldsymbol{M} = \int_{\mathcal{Q}} \boldsymbol{dM}$

Momentum Balance

- Integral form of linear momentum balance:

$$\int_{\partial Q} \boldsymbol{M} = \int_Q \rho \boldsymbol{b} \quad \forall Q \subset D$$

$$\int_Q (\boldsymbol{dM} - \rho \boldsymbol{b}) = \boldsymbol{0} \quad \forall Q \subset D \qquad \text{(Stokes Thm.)}$$

- Local form with jump part:

$$\begin{aligned}(\boldsymbol{dM} - \rho \boldsymbol{b})|_{D \setminus \Gamma^{\mathrm{J}}} &= \boldsymbol{0} \\ [\![\boldsymbol{M}]\!]|_{D \cap \Gamma^{\mathrm{J}}} &= \boldsymbol{0} \rightarrow (\boldsymbol{M}^* - \boldsymbol{M})|_{Q \cap \Gamma^{\mathrm{J}}} = \boldsymbol{0} \\ \boldsymbol{M}^* &= \text{Riemann or prescribed value}\end{aligned}$$

Adaptive refinement

- Refine space mesh using *newest vertex method* to maintain element quality

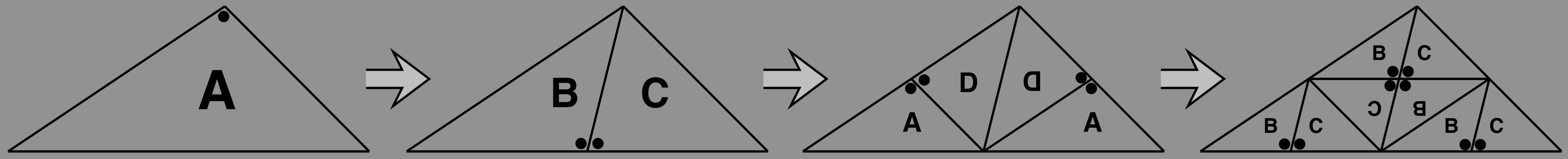

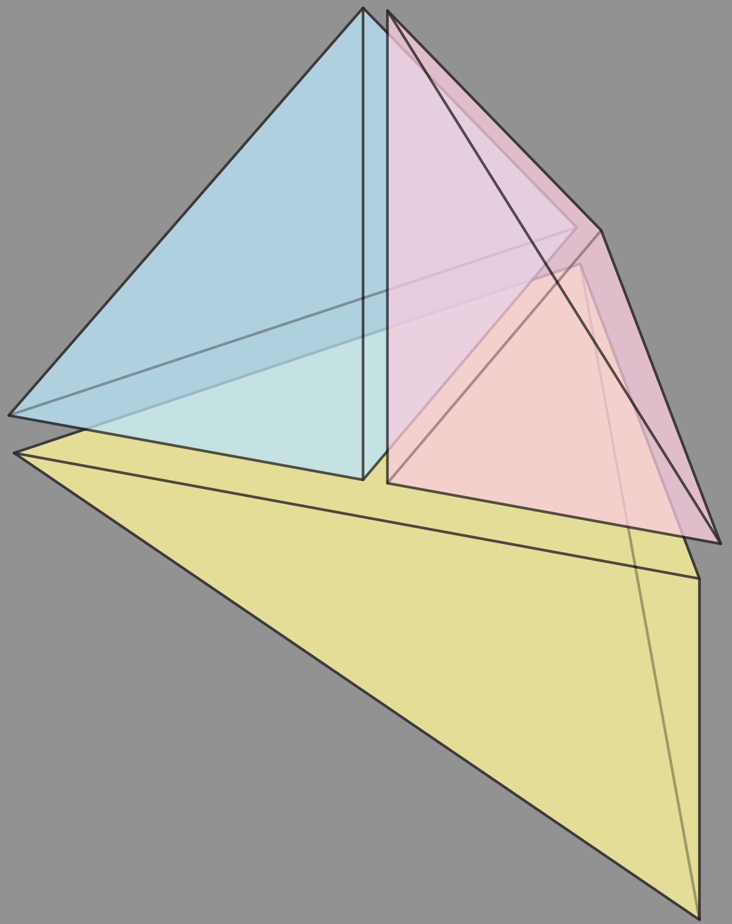

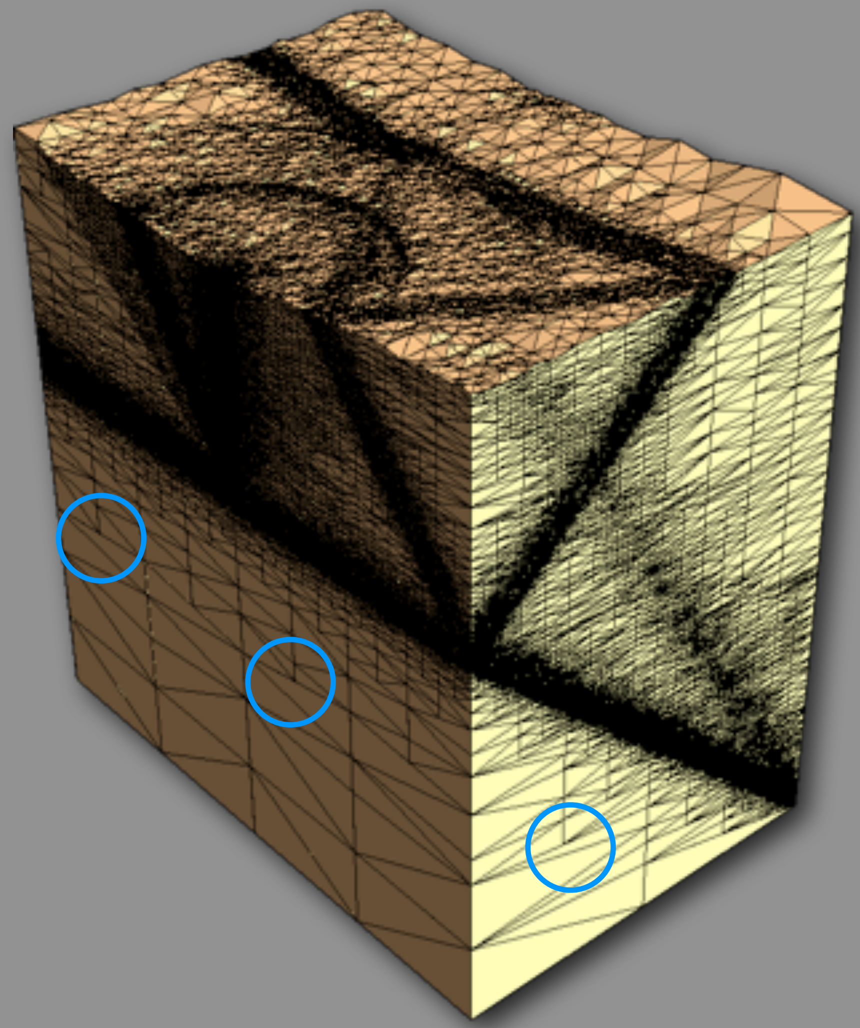

More adaptive meshing

- New spacetime adaptive meshing operations:
  - Edge flip; vertex deletion; inclined tent poles (ALE) for smoothing, tracking and repositioning
  - Spacetime format eliminates projection error

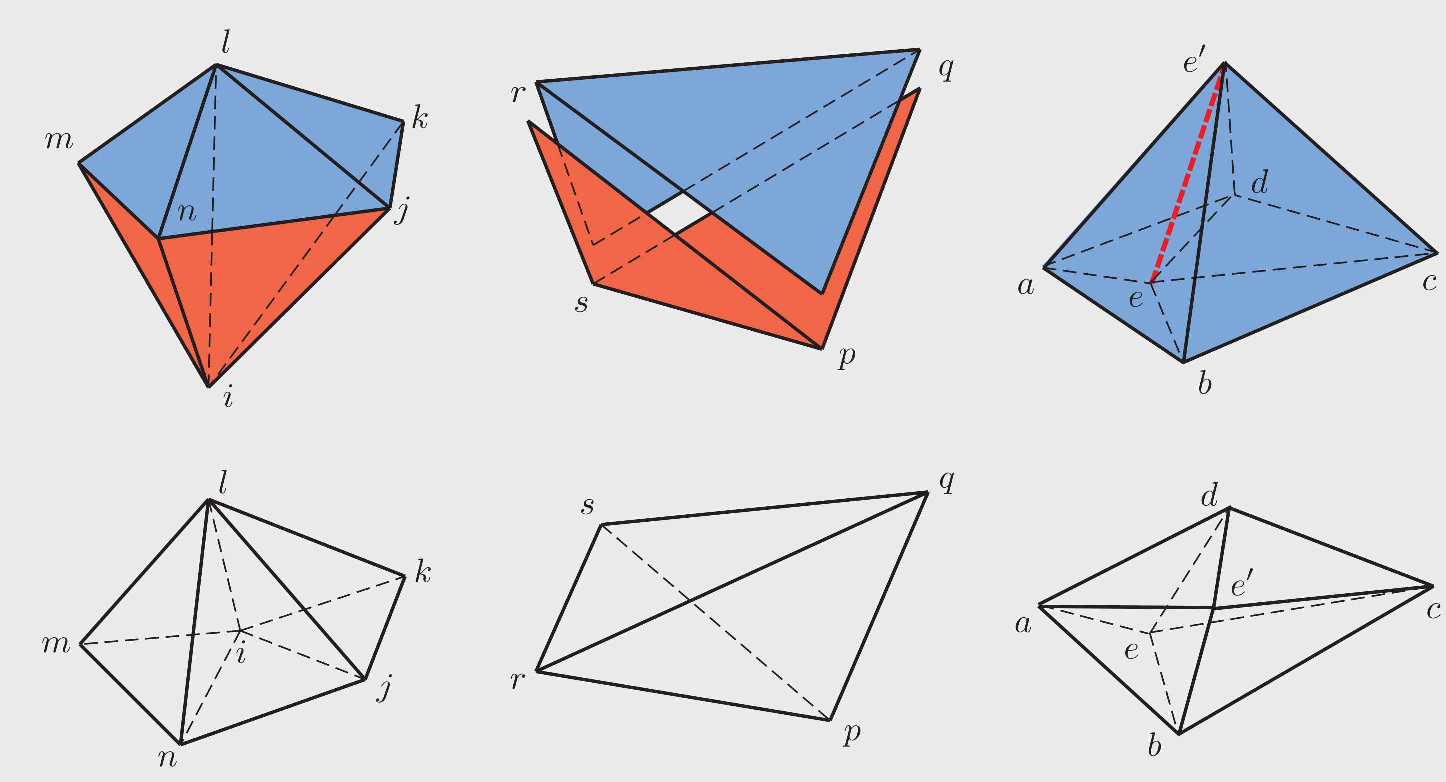

(a) Vertex deletion (degree 5) (b) Edge flip (c) Inclined tent pole

Energy balance and dissipation error indicator for adaptive meshing

- On every spacetime element Q, SDG solution satisfies:

$$\begin{aligned} \varphi^Q &= \int_Q \dot{\mathbf{u}} \wedge \rho \mathbf{b} + \frac{1}{2} \int_{\partial Q} (\dot{\mathbf{u}}^* \wedge \boldsymbol{M}^* + \boldsymbol{\varepsilon}^* \wedge \mathbf{i} \boldsymbol{M}^*) \\ &= \frac{1}{2} \int_{\partial Q} \{(\dot{\mathbf{u}}^* - \dot{\mathbf{u}}) \wedge (\boldsymbol{M}^* - \boldsymbol{M}) + (\boldsymbol{\varepsilon}^* - \boldsymbol{\varepsilon}) \wedge \mathbf{i}(\boldsymbol{M}^* - \boldsymbol{M})\} \end{aligned}$$

  Right hand side is non-negative numerical dissipation for Q.

- To control adaptively the numerical dissipation, we use the element-wise error indicator:

$$\varphi^Q \approx \mathrm{tol}_\varphi$$

Cohesive error measure and adaptive error indicator

- Cohesive energy error on cohesive surface trajectory, Γ^{C}:

$$\epsilon_{\mathrm{C}} = \|(\mathbf{t} - \mathbf{t}_{\mathrm{coh}}) \cdot \mathbf{v}\|_{L_1(\Gamma^{\mathrm{C}})}$$

- Cohesive error indicator for element Q:

$$\epsilon_{\mathrm{C}}^{Q} = \|(\mathbf{t} - \mathbf{t}_{\mathrm{coh}}) \cdot \mathbf{v}\|_{L_1(\partial Q_{\mathrm{coh}})} \approx \mathrm{tol}_{\mathrm{c}}$$

Crack-tip Wave Scattering

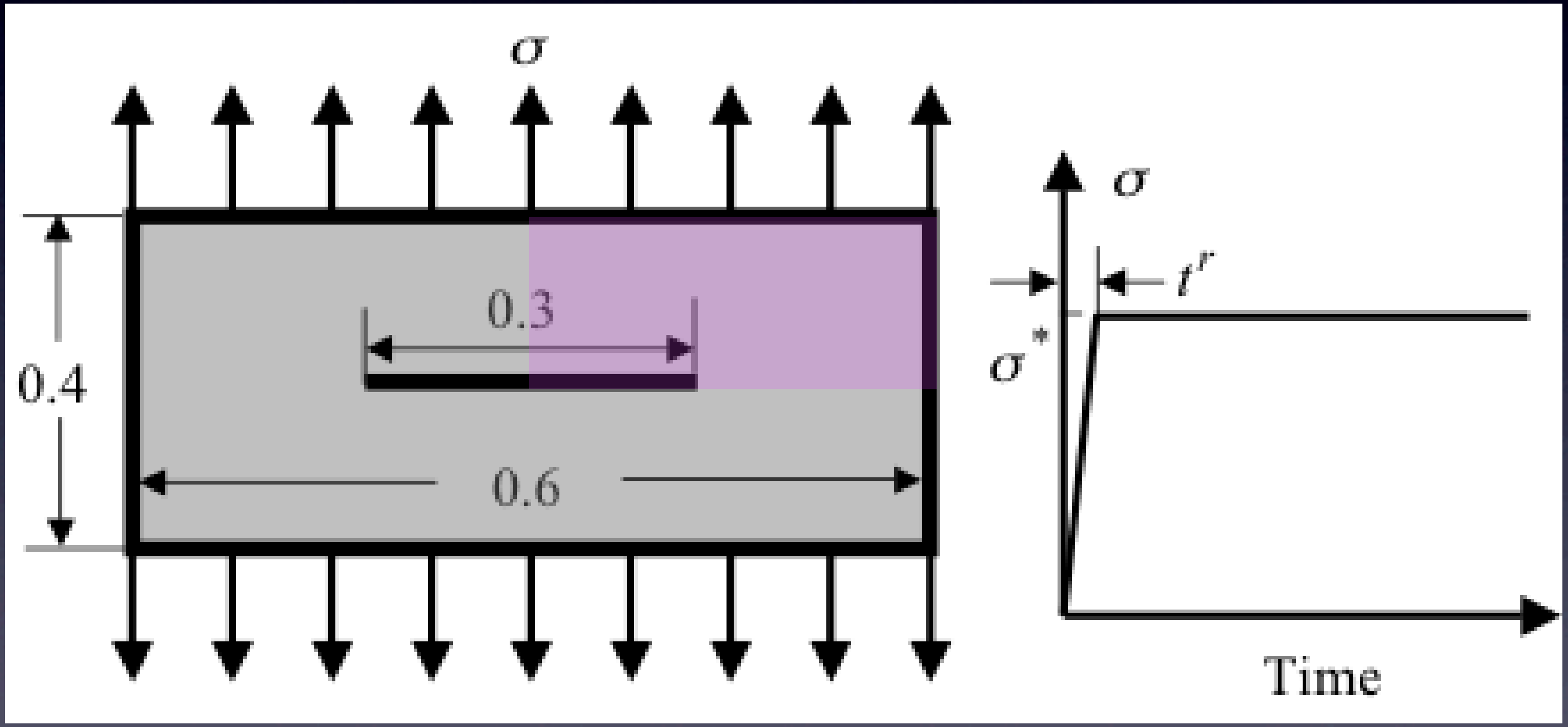

Crack-tip Wave Scattering

click to play movie

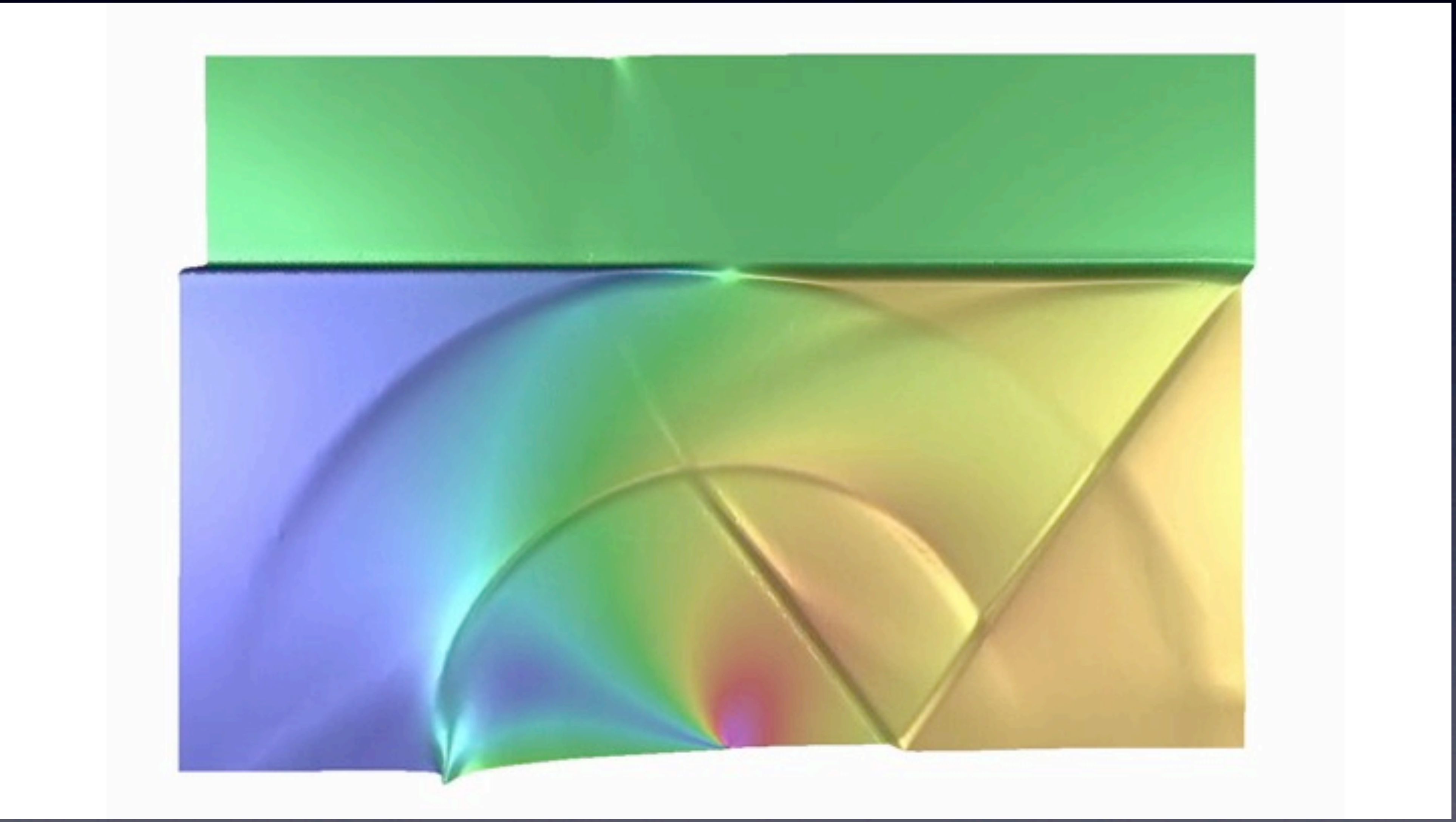

Crack-tip Wave Scattering

click to play movie

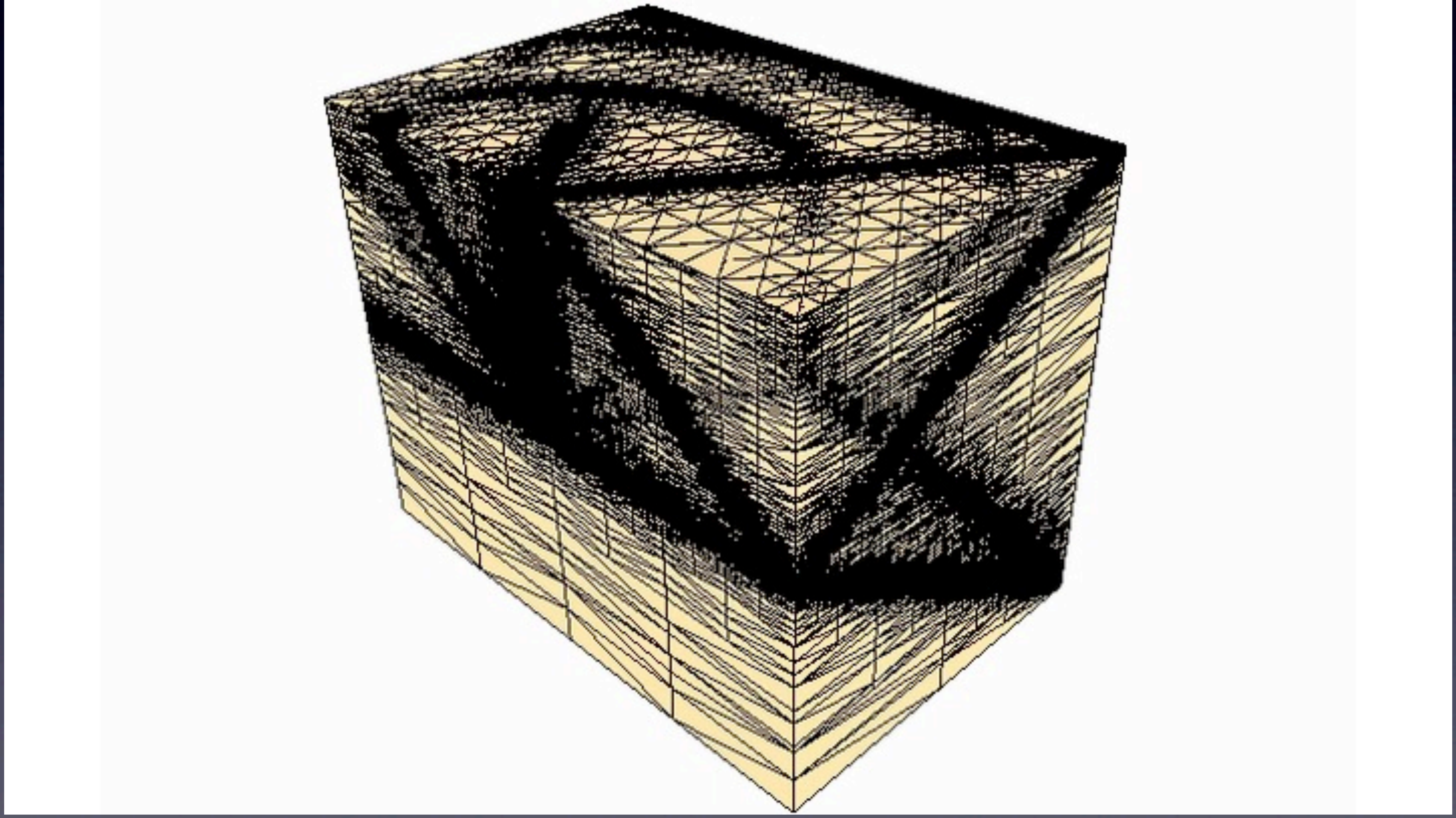

Crack-tip Wave Scattering

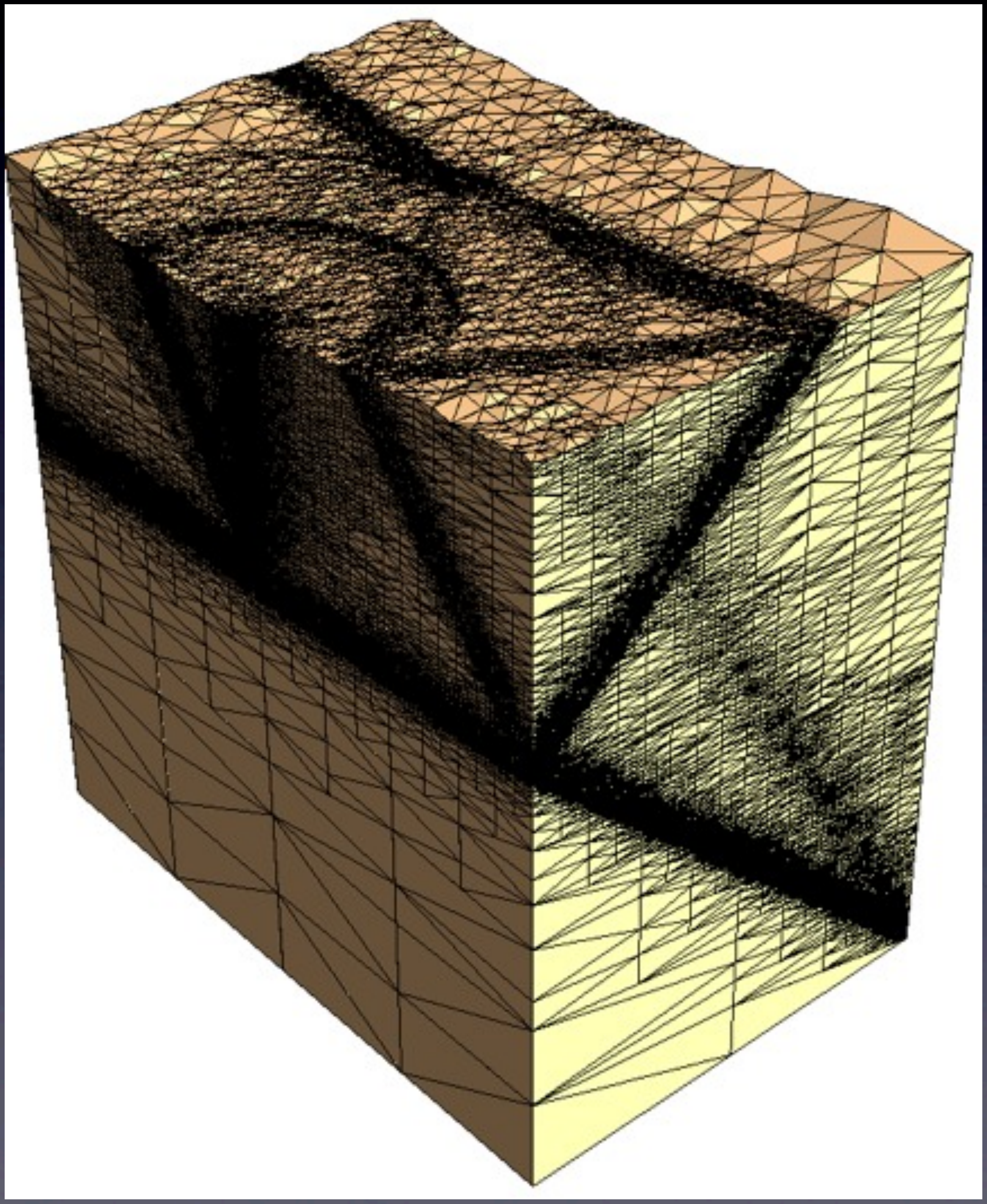

Delay Damage Evolution Cohesive Model

$D = \text{Area fraction of debonded surface}$

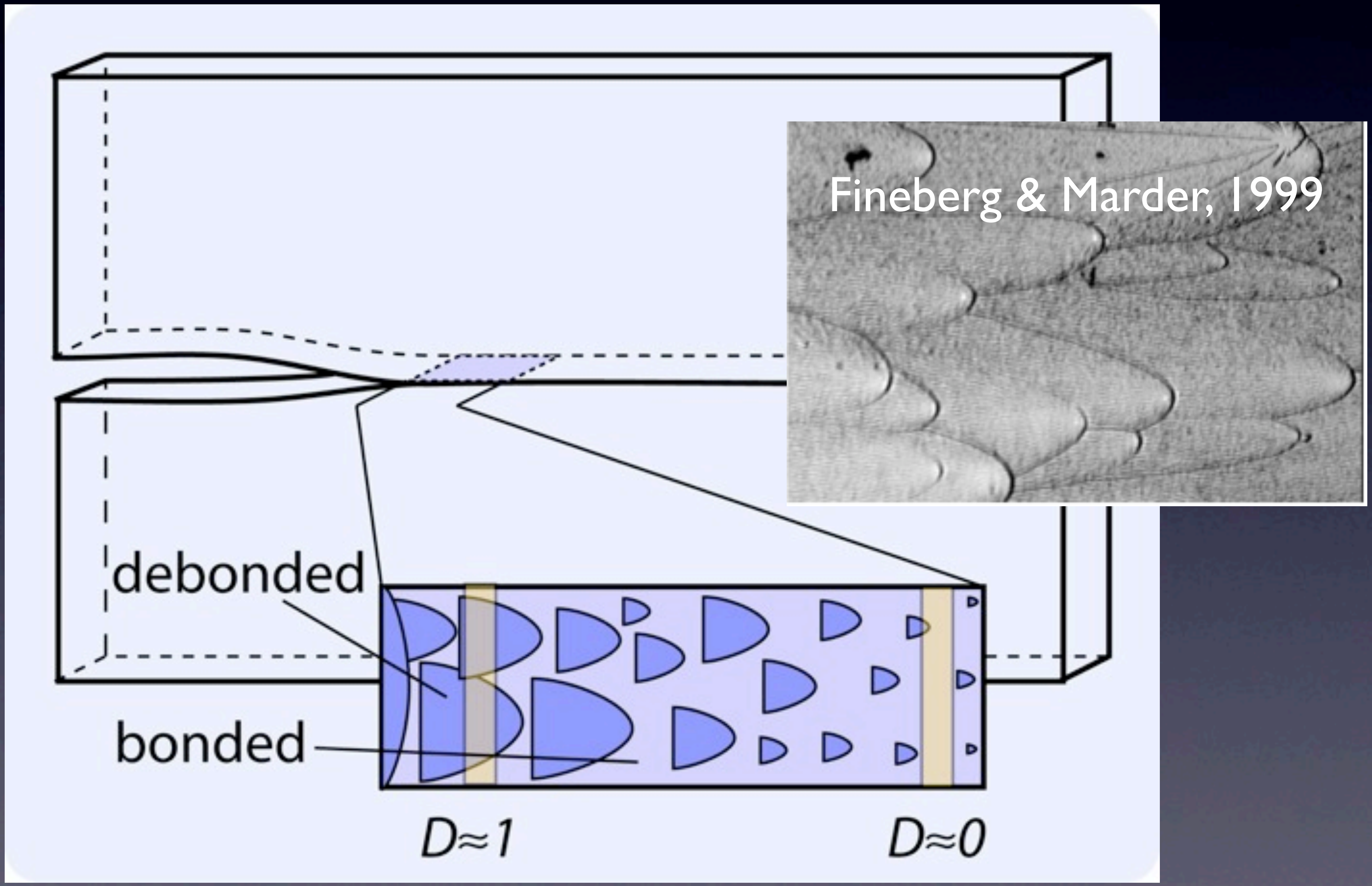

Mesoscopic interface subdivisions

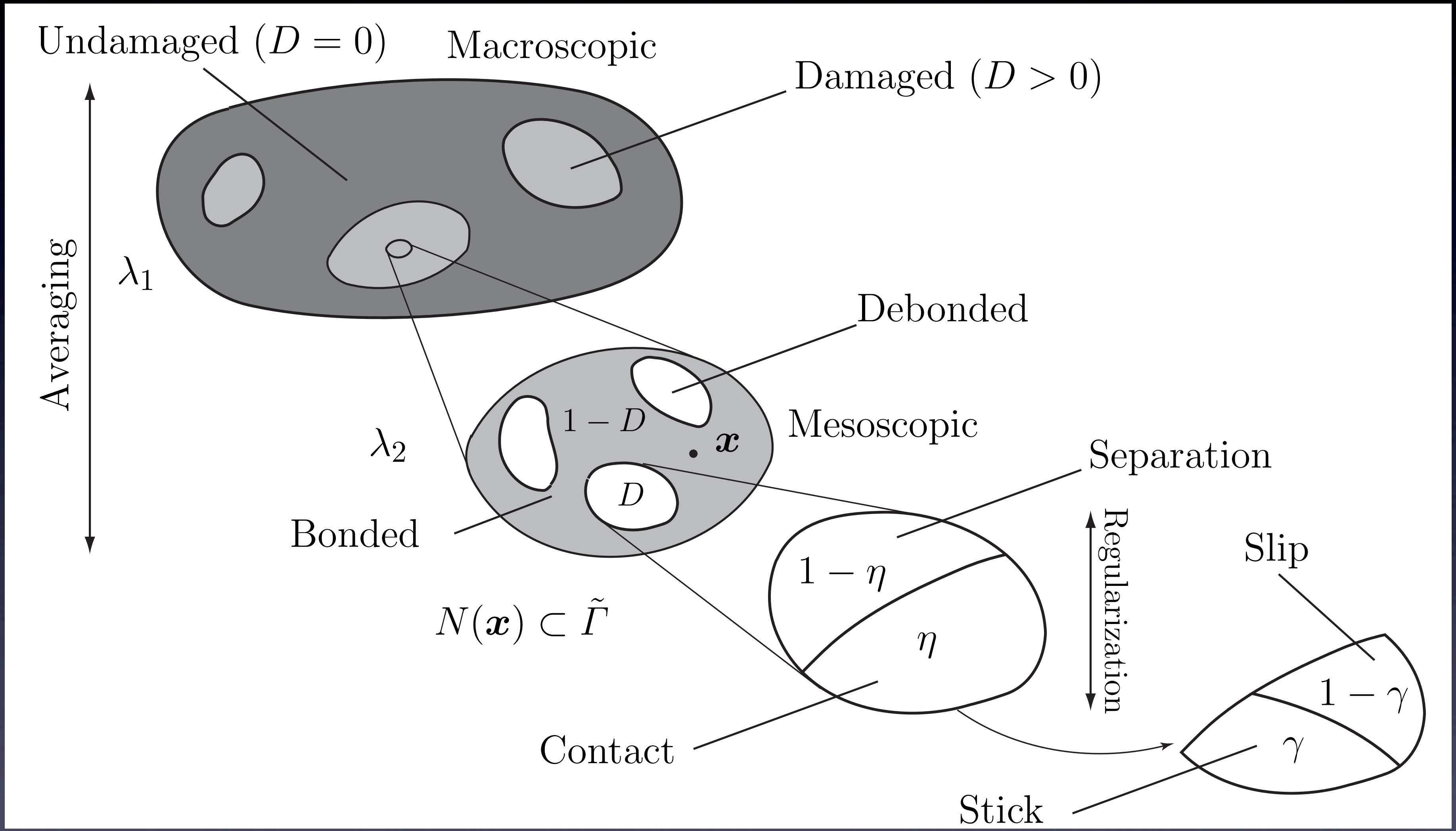

Contact conditions

- Common numerical idealizations of contact
  - ✦ Discrete models - goal is to prevent node penetration
  - ✦ Elastostatic contact conditions
  - ✦ Penalty methods and other inexact formulations
    - $\mathbf{s} = f(\Delta\mathbf{u}) = \; K\Delta\mathbf{u}(\Delta\mathbf{u} < 0)$ but $\Delta\mathbf{u} = 0!$
    - Approach exact solution for large K $\Rightarrow$ divergence
  - ✦ Variational Inequality/Lagrange multiplier methods
    - Lagrange variables increase the problem size
    - typically require an implicit solution scheme

Riemann Contact/Separation Solutions

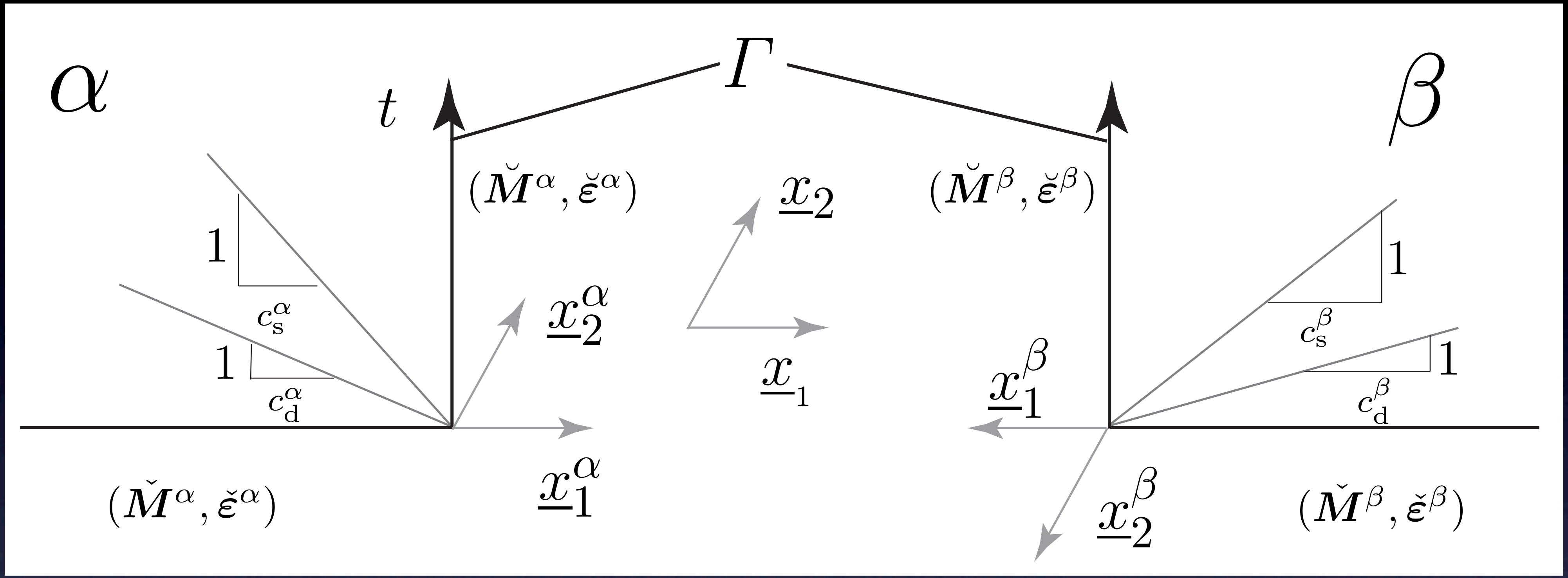

- Direct solution from momentum balance and compatibility jump conditions
- Matching conditions at material interface
- Preserves characteristic structure of solution
- Weak enforcement of the continuum, dynamic jump conditions converges to correct result

Interface Matching condition
Bonded and contact-stick

- Matching conditions
  - Momentum: $[\![\breve{\mathbf{s}}]\!] = 0$
  - Compatibility: $[\![\breve{\mathbf{v}}]\!] = 0$
- Riemann Solution
  - $\underline{s}^{j^I} = [\![\underline{w}^{(j)}/\rho\underline{c}^{(j)}]\!]/[\![(\rho\underline{c}^{(j)})^{-1}]\!]$
  - $\underline{v}_j^I = [\![\underline{w}^{(j)}]\!]/[\![(\rho\underline{c}^{(j)})^{-1}]\!]$
- Contact-stick and bonded solutions are identical
- Contact-stick and separation solutions are physically distinct:
  - Contact-stick
  - Separation

Contact-stick:

$$\Delta\mathbf{u} = \mathbf{0}$$

$$\mathbf{s} = ?$$

Separation:

$$\Delta\mathbf{u} = ?$$

$$\mathbf{s} = \mathbf{0} \quad or \quad \mathbf{s} = f(\Delta\mathbf{u})(TSL)$$

Interface Matching condition
Contact-slip

- Matching conditions
  - Momentum: $[\![\breve{\mathbf{s}}]\!] = 0$
  - Compatibility: $[\![\breve{\underline{v}}_1]\!] = 0$
  - Coulomb's law: ${\underline{s}^j}^{II} = k\langle -\underline{s}^1_I\rangle_+ (e_{\breve{\mathbf{v}}})^j \;\; j \neq 1$
- Riemann Solution

$$
{\underline{s}^j}^{II} = \begin{cases} {\underline{s}^1}^I & j = 1 \\ k\langle -\underline{s}^1_I\rangle_+ (e_{\boldsymbol{\tau}_I})^j & j \neq 1 \end{cases}
$$

$$
\underline{v}^{II}_j = \begin{cases} \underline{v}^I_1 & j = 1, \\ \underline{w}^{(j)}/\rho\underline{c}^{(j)} - {\underline{s}^j}^{II}/\rho\underline{c}^{(j)} = \breve{\underline{v}}_j + \left(\breve{\underline{s}}^j - {\underline{s}^j}^{II}\right)/\rho\underline{c}^{(j)} & j \neq 1 \end{cases}
$$

- Slip velocity $[\![\breve{\mathbf{v}}]\!] \to \mathbf{0}$ at stick-slip transition $\Rightarrow$ Discontinuous response from $(e_{\breve{\mathbf{v}}})^j$
- many regularizations proposed to solve the problem (Karnopp, Mostaghel, Quinn)
- $\boldsymbol{\tau}_I > 0$ at stick-slip transition $\Rightarrow$ Continuous response from $\boldsymbol{\tau}_I > 0$

Interface Matching condition Separation

- Matching conditions
  - Momentum and constitutive equation: $\breve{\mathbf{s}} = \mathbf{0}$
  - No compatibility condition
- Riemann Solution
  - $\mathbf{s}^{III} = \mathbf{0}$
  - $\underline{v}_j^{III} = \frac{\underline{w}^{(j)}}{\rho \underline{c}^{(j)}}$

Mesoscopic subdivision
Damaged area (D)

- General Properties of Damage parameter
  - ✦ Nondecreasing (irreversible process)
  - ✦ Stress Induced (Ravi-Chandar, Yang 1997)
  - ✦ Exact Bonded solution is recovered for D = 0
  - ✦ Stress free (crack) surface condition at D = 1
- Rate Dependent damage model
  - ✦ Hardening effects at high strain rates (experimental results from Fineberg and Marder 1999)
  - ✦ Introduces a fracture related length scale
  - ✦ Mesh dependency of static damage models (strain softening failure, Bazant and Belytschko 1984)

Damage Evolution

Follow delay damage evolution model of Allix, Feissel and Thévenet:

$$\tilde{\sigma} = \frac{\sqrt{\sigma_{\mathrm{N}}^2 + (\beta\sigma_{\mathrm{T}})^2}}{\sigma_{\mathrm{c}}}$$ normalized effective stress

$$\bar{D} = f(\tilde{\sigma})$$ static damage value

$$\dot{D} = \begin{cases} \frac{1}{\tau}\left[1 - H(\langle f(\tilde{\sigma}) - D\rangle_+)\right] \text{ if } D < 1 \\ 0 \text{ if } D = 1 \end{cases}$$ damage evolution law

where τ is a *characteristic time scale* for debonding, and $H(0) = 1$ and $\lim_{x\to\infty} H(x) = 0$. We use

$$H(x) = e^{-ax}$$

This model implies

$$D = \bar{D} \Rightarrow \dot{D} = 0$$

Mesoscopic subdivision
Contact area (η)

- Contact/Separation transition may introduce shocks in tractions and velocities
- Regularization is required for shock capturing schemes
- Regularization is based on normal contact traction and macroscopic traction
- A minimum separation value of r_c is ensured in the regularized model
- Surface toughness may provide physical regularization
- No regularization is required for stick-slip areas

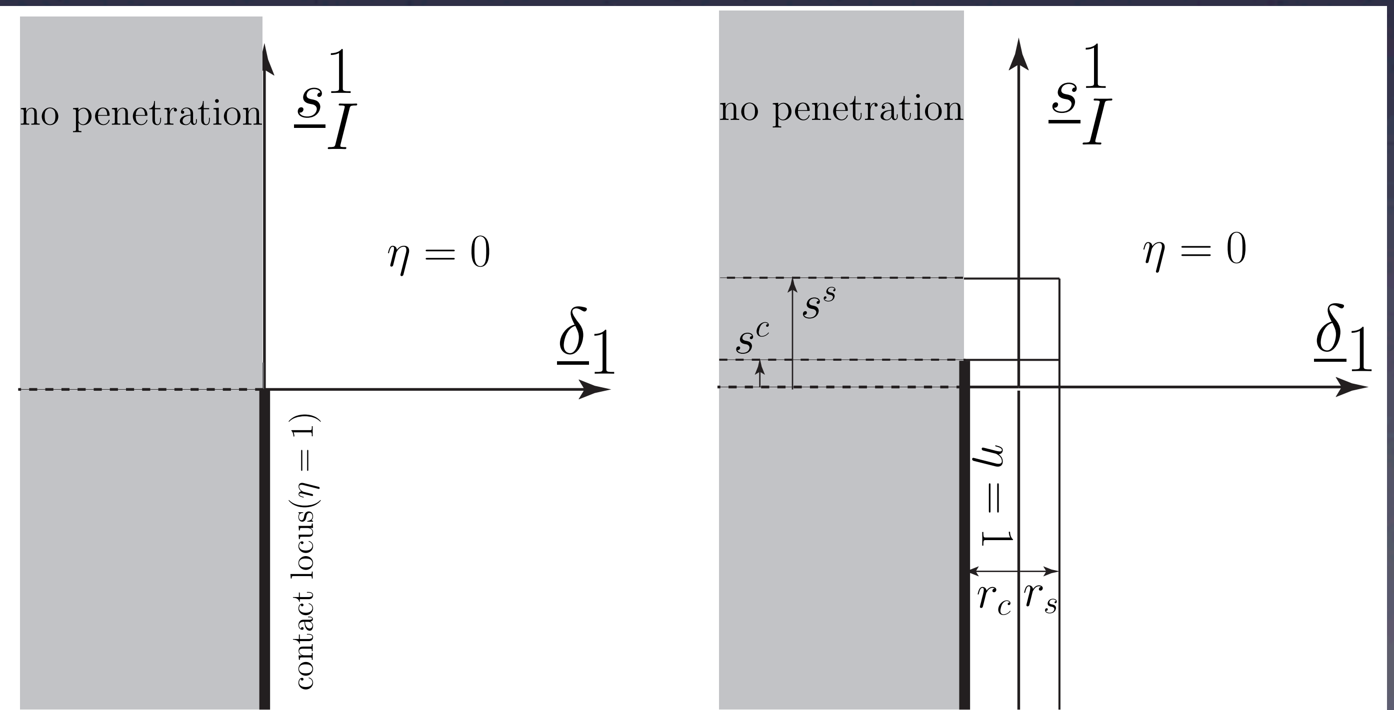

(a) Contact scheme prior to regularization.

(b) Regularized contact scheme.

Crack closure example: brittle fracture under cyclic, dynamic loading conditions

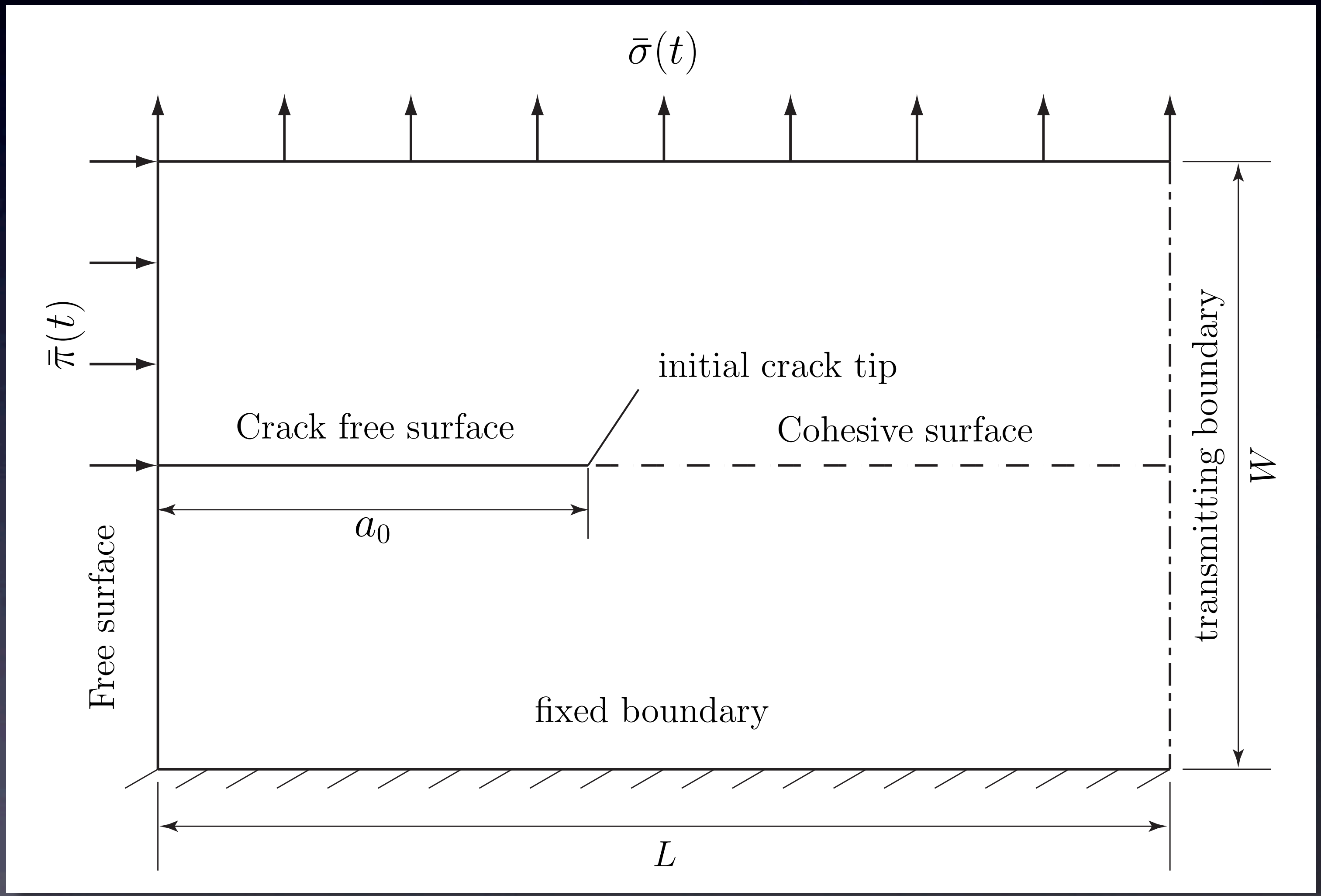

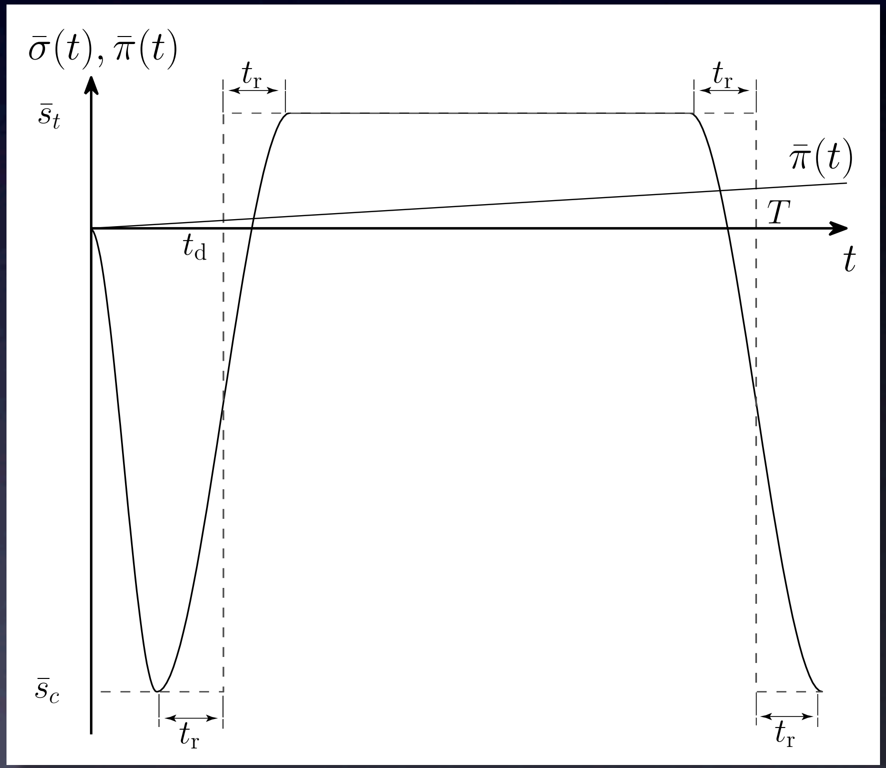

Crack closure example: brittle fracture under cyclic, dynamic loading conditions

click to play movie

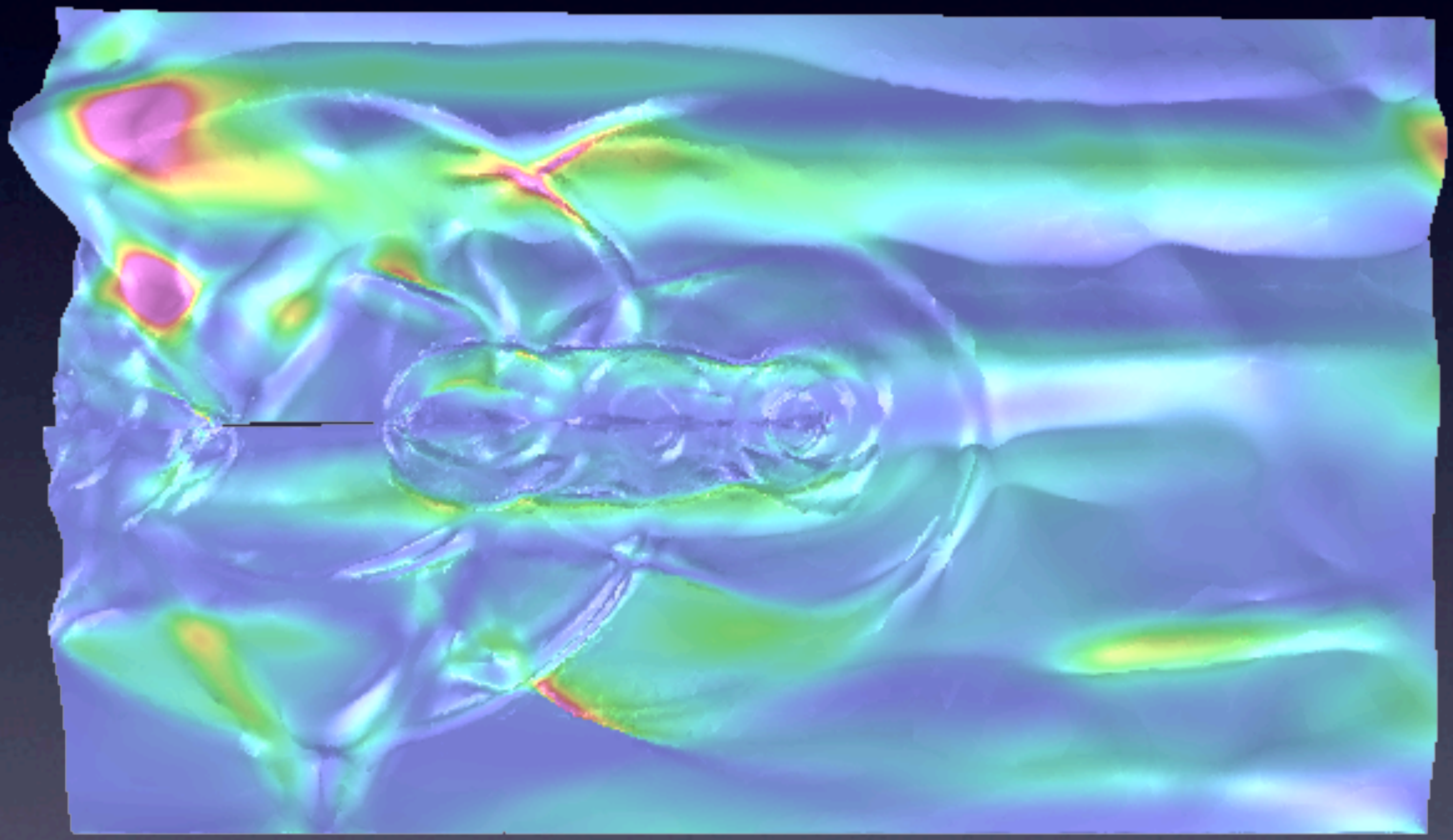

Solution-dependent crack paths

- Inclined tent poles, edge bisection and smoothing extend cohesive zone in any desired direction
- Effective stress criterion for extending cohesive surface
  - maximum value determines direction for extension
- Nucleation + coalescence = branching
  - Probabilistic nucleation criterion models random defects
  - Introducing cohesive surface does not affect behavior until damage accumulates

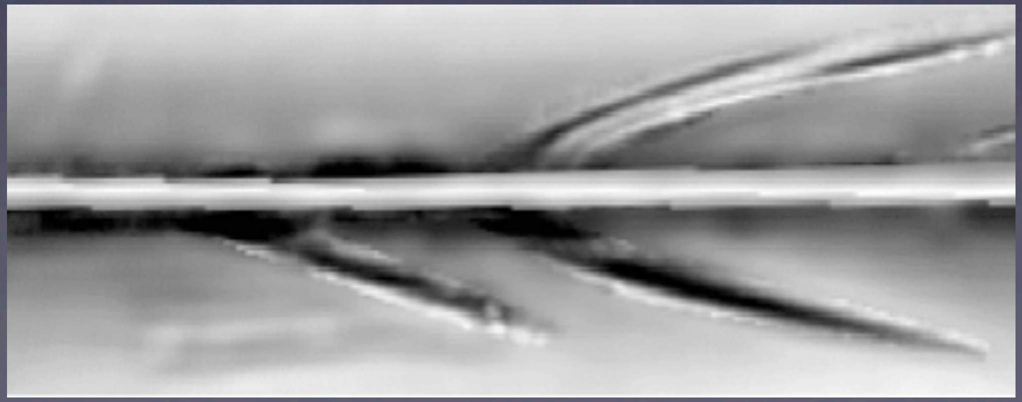

Solution-dependent crack propagation Geometry and Loading

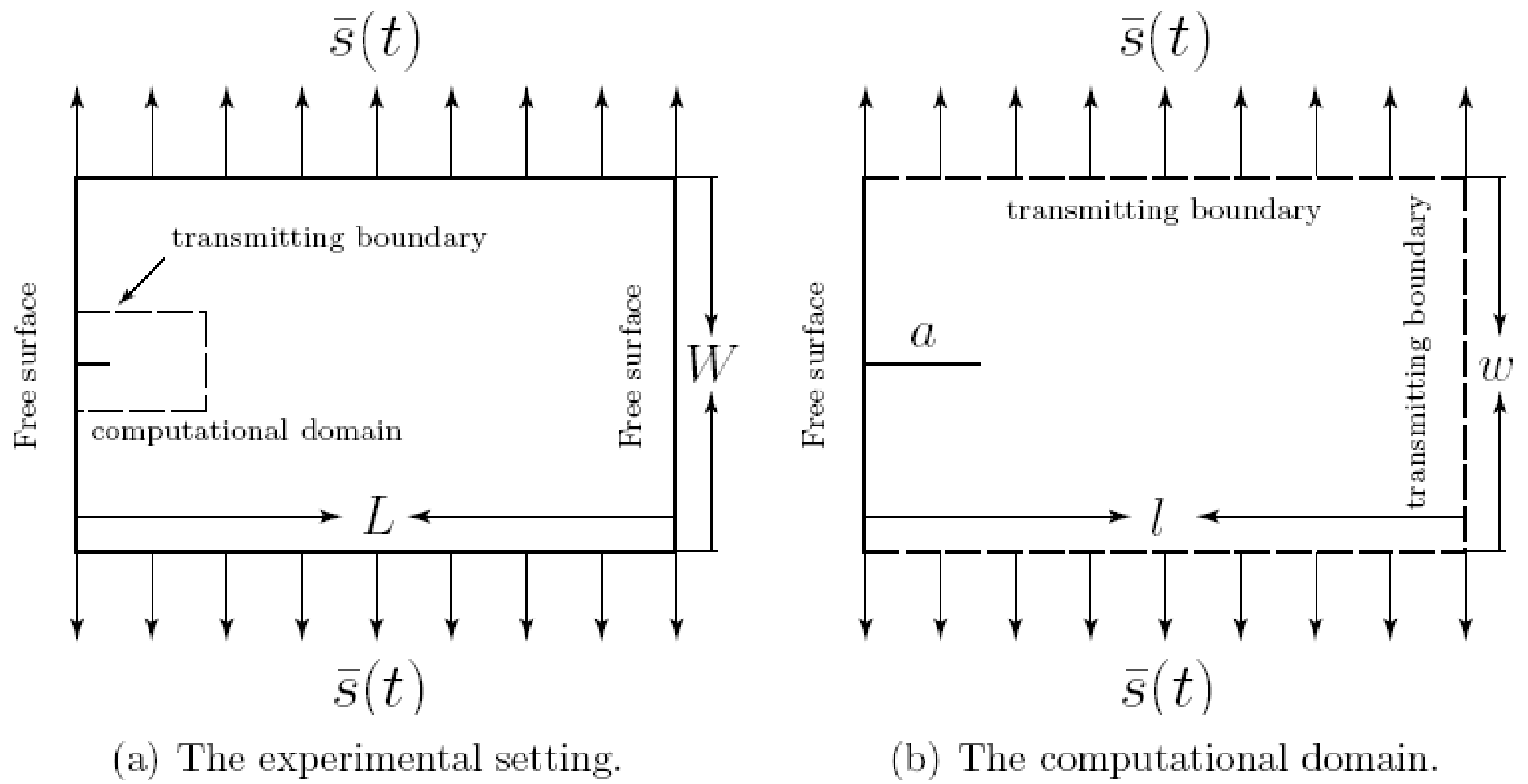

PMMA:

- $E = 3.24GPa$.
- $\rho = 1190\frac{Kg}{m^3}$.
- $w = 0.020MPa$.
- $\tau = 10^{-2}\mu s$.

based on Sharon and Fineberg experiment (1996)

Refinement Details: 1 x zoom

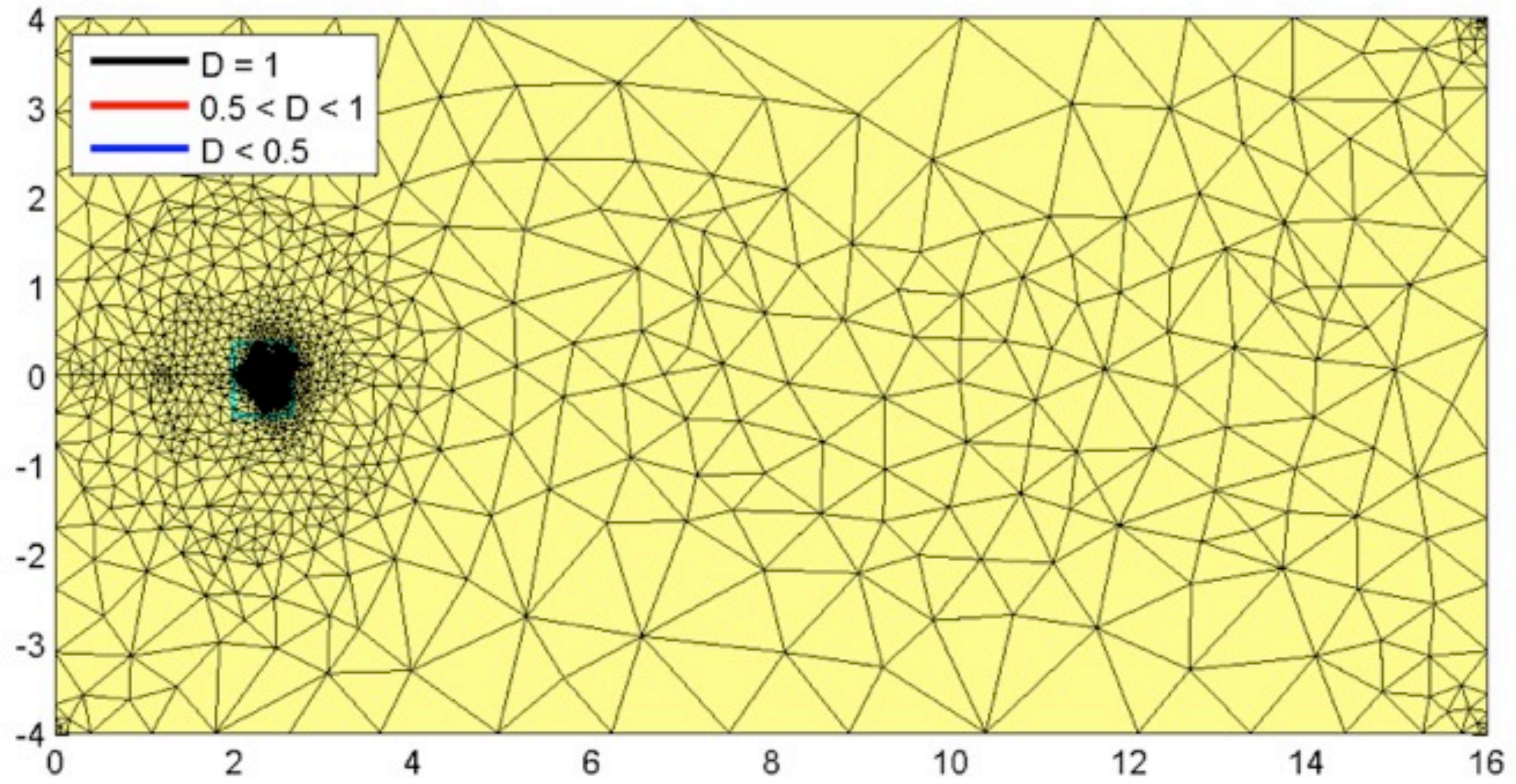

Refinement Details: 25 x zoom

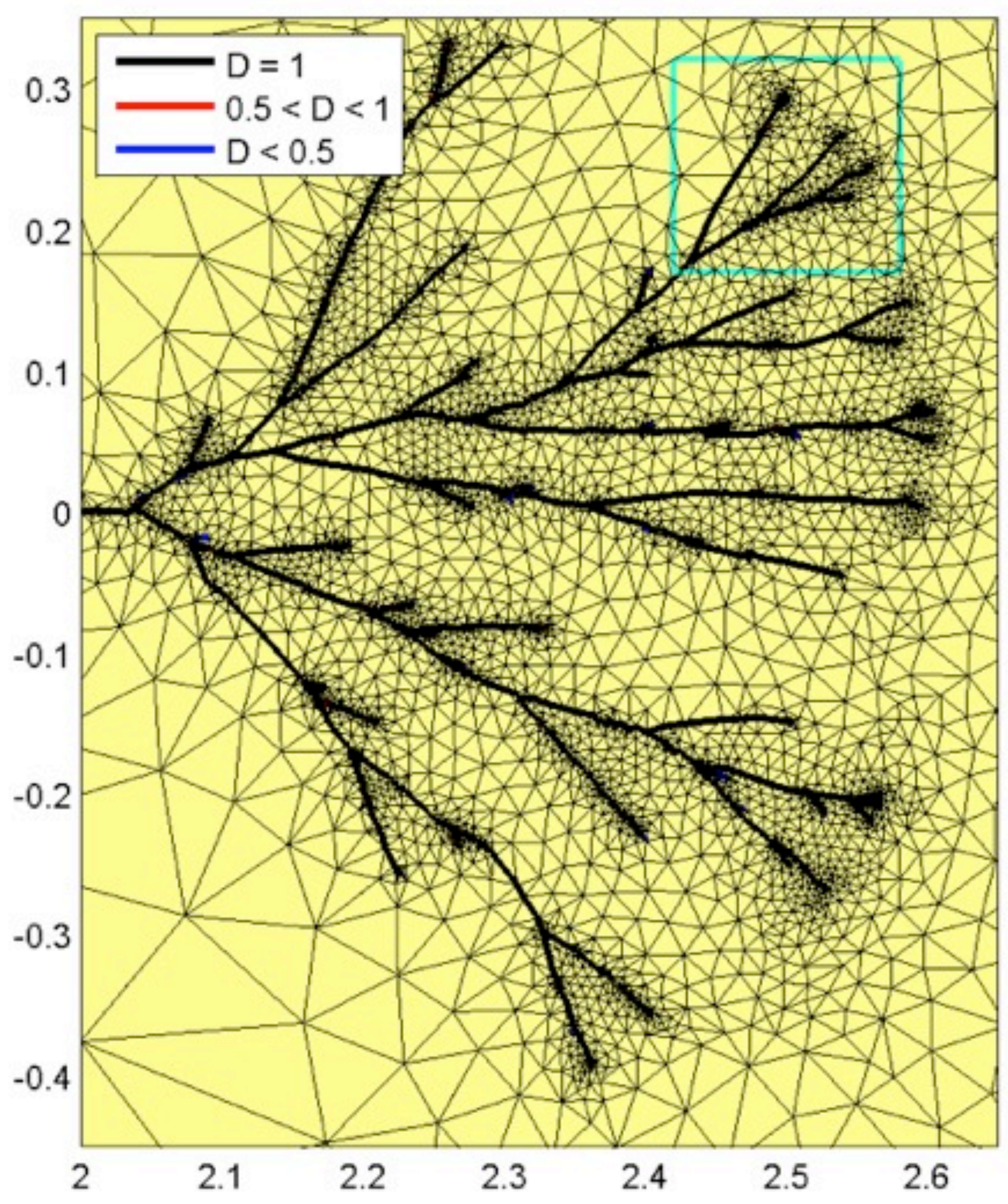

Refinement Details: 100 x zoom

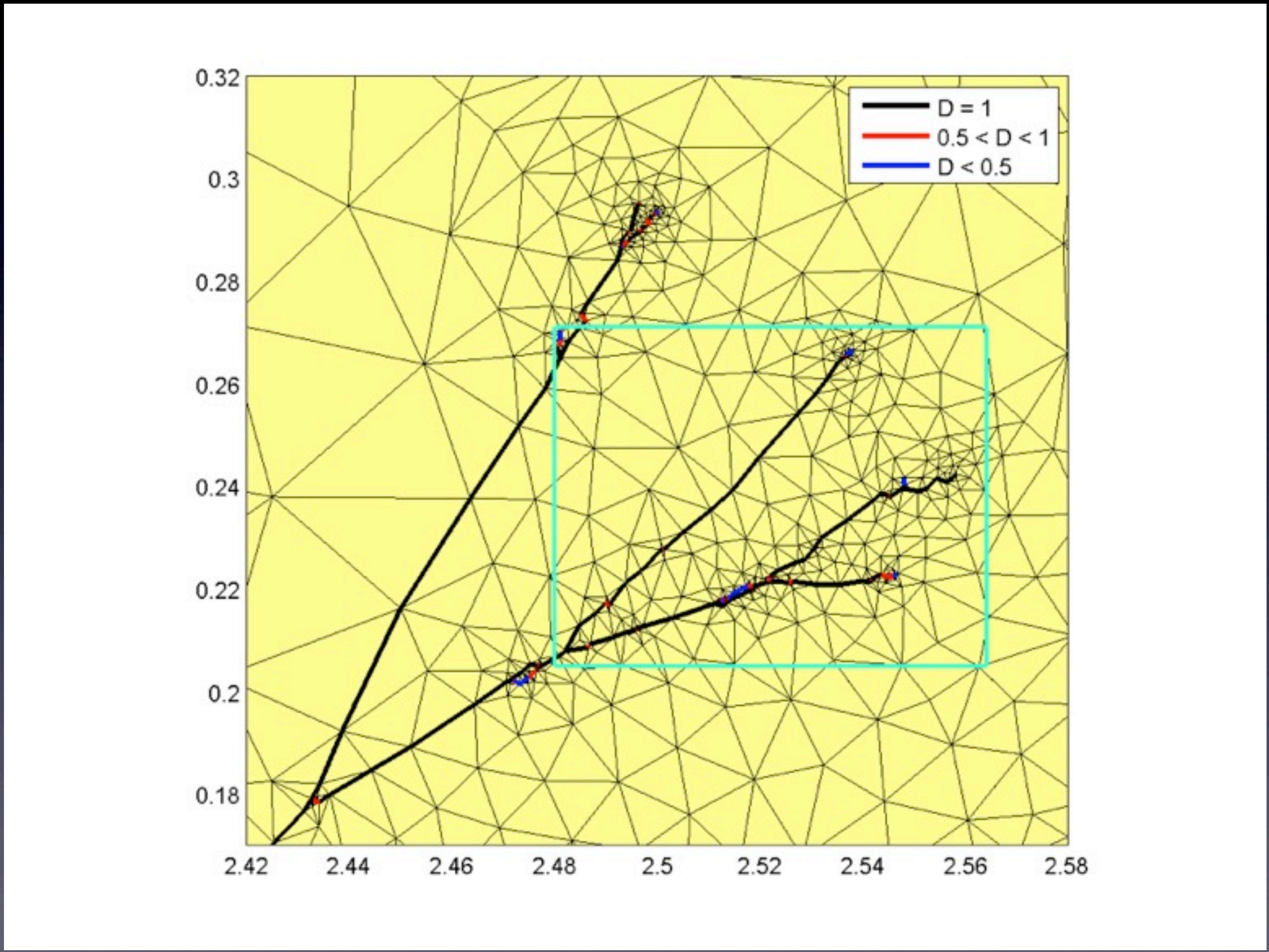

Refinement Details: 200 x zoom

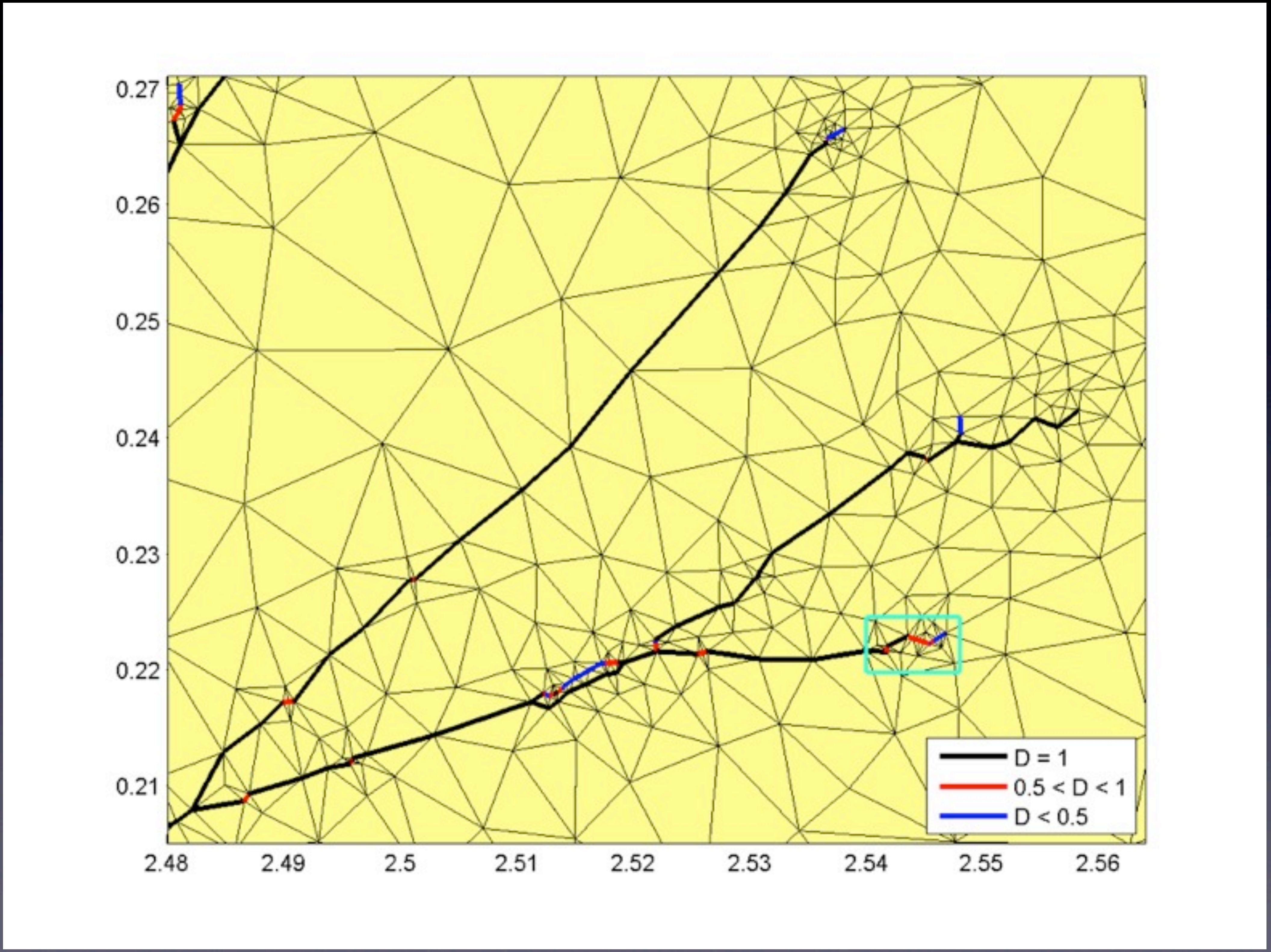

Refinement Details: 2000 x zoom

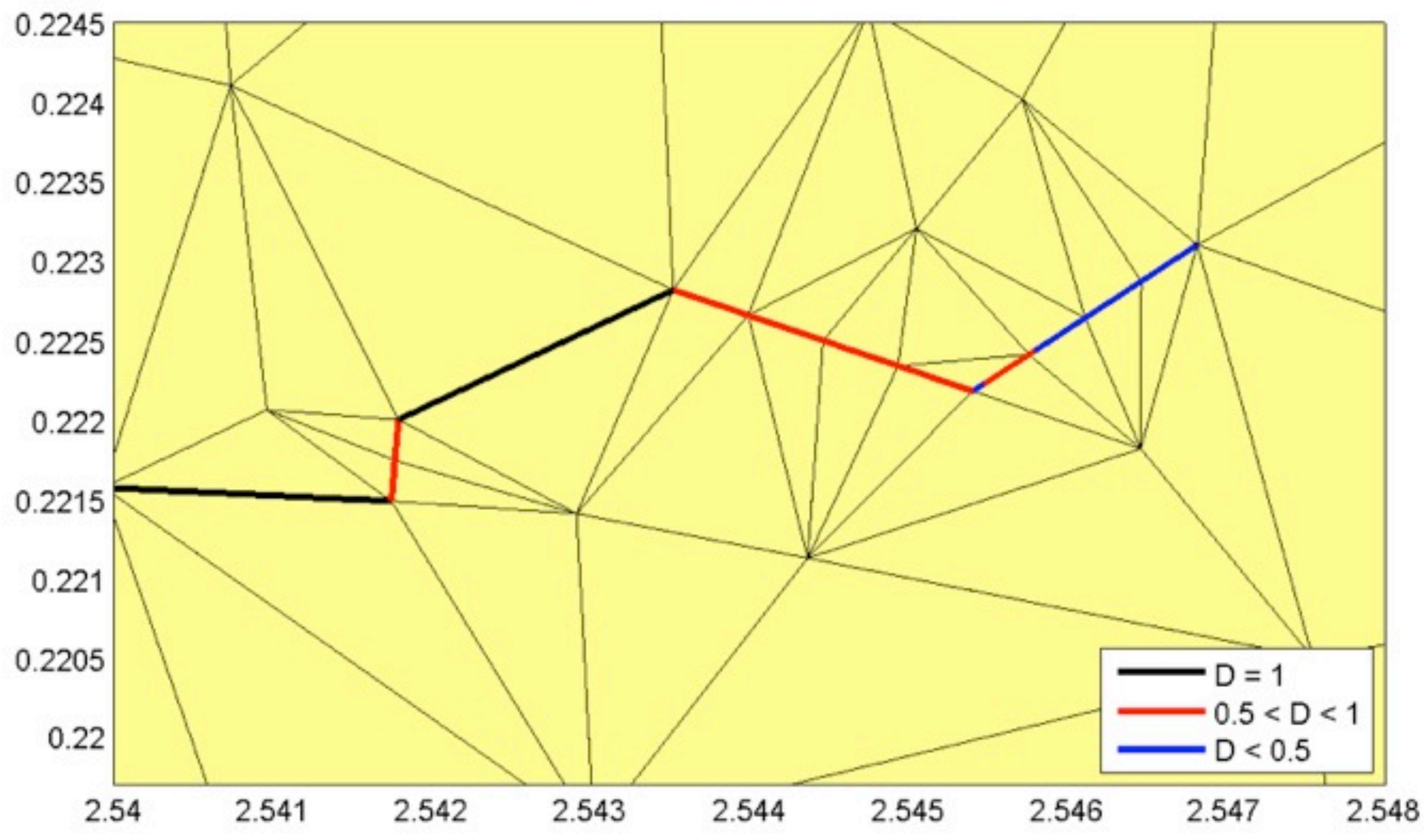

Same problem with crack closure contact model, random defects and nucleation

click to play movie

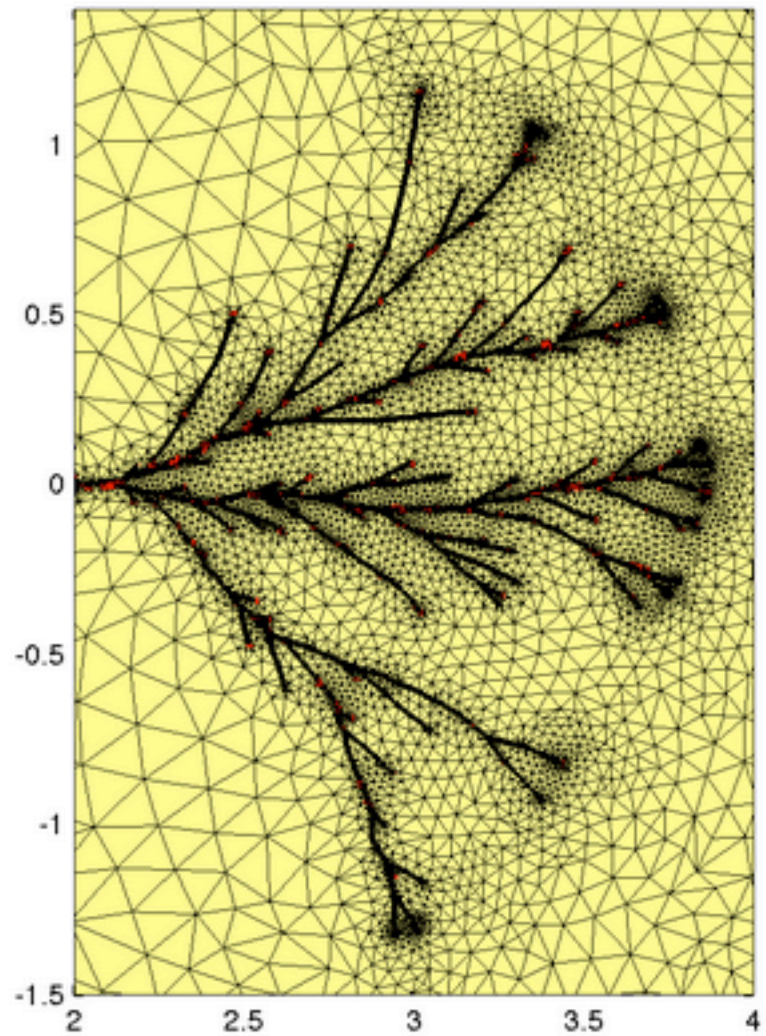

Effect of contact conditions on crack path

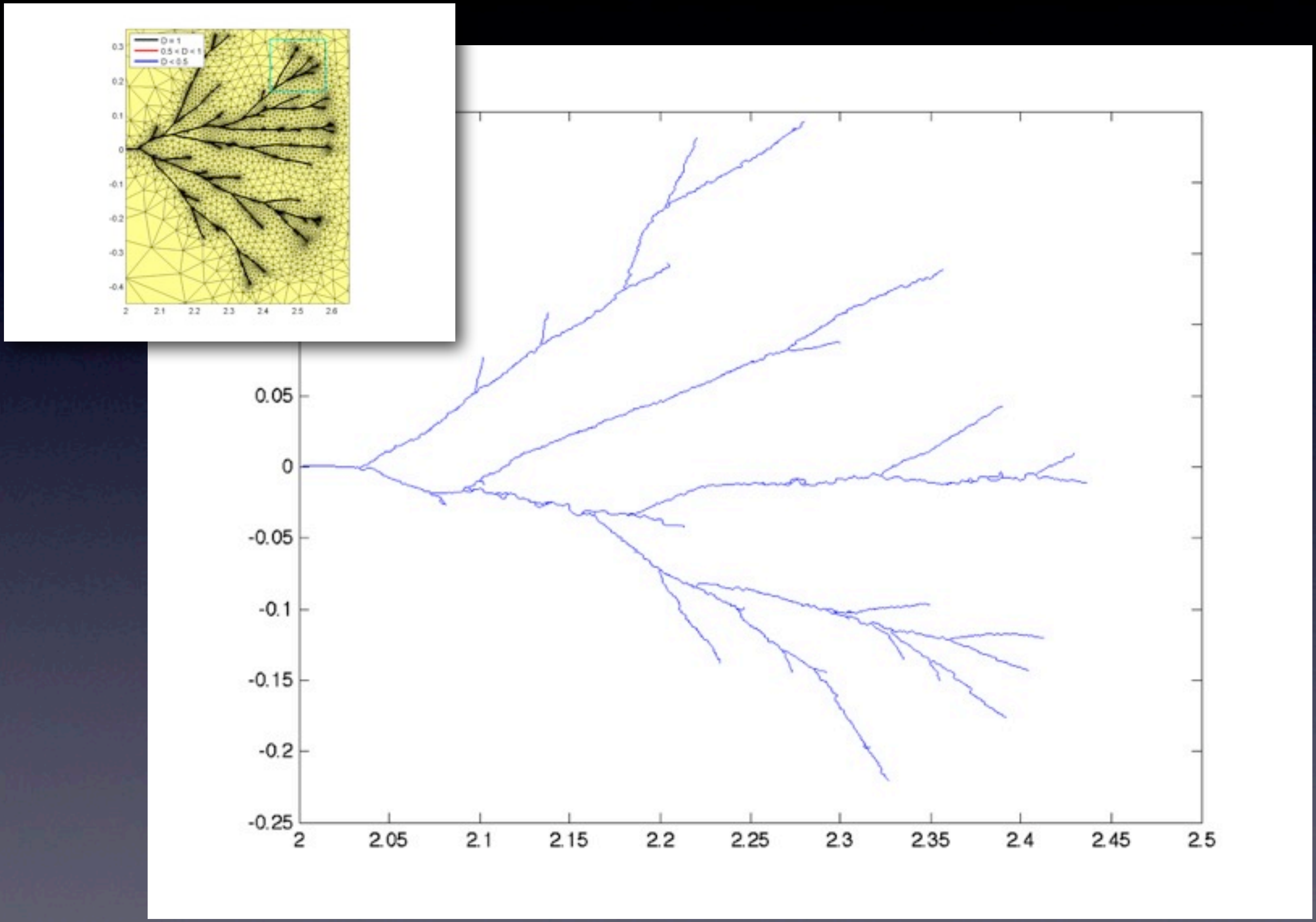

Surface roughening at high crack velocities

- Almost uniform hoop stress distribution at $\dot{a} > 2/3 c_{\mathrm{R}}$ (Yoffe, 1951)
- Experimentally observed roughness on crack surface (Smekal, 1953; Kerkhof, 1973; Sharon and Fineberg, 1996)
- Surface roughening and branching instabilities in dynamic fracture; Phenomenological wavy crack path (Gao, 1992)
- Dynamical stability of a propagating crack: Obrezanova (2002) at $\dot{a} > 1/3 c_{\mathrm{R}}$ crack may admit one or more oscillatory modes of instability
- Stability of dynamically propagating cracks in brittle materials: Uenishi *et. al.* (2001): Surface roughness induced by increase of crack velocity

Single crack velocity agreement with experiments

- Material degradation and energy loss due to induced heat should be contributed in the model (Sharon and Fineberg 1996)
- Bulk material dissipative and damage models to be incorporated
- Material degradation around the crack tip, the high inertia zone, and subsequent drop in wave speed (Ravi *et. al.*, 2007)
- Surface tension or hardness in computing the limiting velocity, Kerkhof (1997)

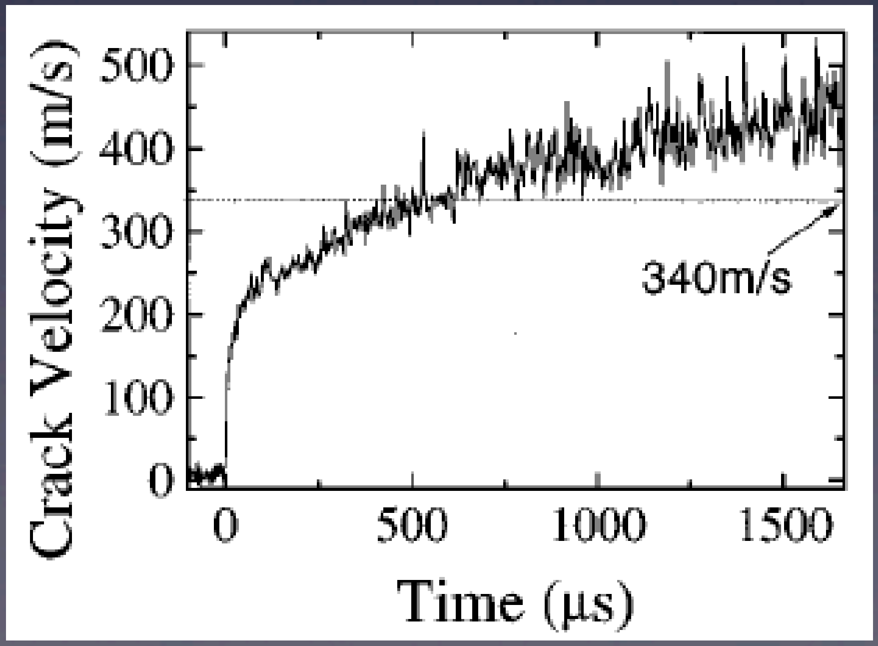

Summary

- Robust adaptive model for crack growth
  - Ensures accurate rendering of cohesive models
  - Eliminates all mesh-dependence effects
  - Supports nucleation
  - Captures multi-scale behavior
  - Captures the details of crack propagation (Branching, micro branching, surface roughening)
- New dynamic, continuum contact formulation
- Open physical modeling issues
  - Crack acceleration too rapid (typical of cohesive models)
  - Branching pattern does not completely match experiment
  - Some aspects heuristic, but have framework for developing